



**HAL**  
open science

## Geodynamics of the northern Andes: Subductions and intracontinental deformation (Colombia)

Alfredo Taboada, Luis Rivera, Andrés Fuenzalida, Armando Cisternas, Hervé Philip, Harmen Bijwaard, José Olaya, Clara Rivera

► **To cite this version:**

Alfredo Taboada, Luis Rivera, Andrés Fuenzalida, Armando Cisternas, Hervé Philip, et al.. Geodynamics of the northern Andes: Subductions and intracontinental deformation (Colombia). *Tectonics*, 2000, 19 (5), pp.787-813. 10.1029/2000TC900004 . hal-03257427

**HAL Id: hal-03257427**

**<https://hal.science/hal-03257427>**

Submitted on 11 Jun 2021

**HAL** is a multi-disciplinary open access archive for the deposit and dissemination of scientific research documents, whether they are published or not. The documents may come from teaching and research institutions in France or abroad, or from public or private research centers.

L'archive ouverte pluridisciplinaire **HAL**, est destinée au dépôt et à la diffusion de documents scientifiques de niveau recherche, publiés ou non, émanant des établissements d'enseignement et de recherche français ou étrangers, des laboratoires publics ou privés.

Copyright

## Geodynamics of the northern Andes: Subductions and intracontinental deformation (Colombia)

Alfredo Taboada,<sup>1,2</sup> Luis A. Rivera,<sup>3,4</sup> Andrés Fuenzalida,<sup>5</sup> Armando Cisternas,<sup>4</sup>  
Hervé Philip,<sup>1</sup> Harmen Bijwaard,<sup>6</sup> José Olaya,<sup>5</sup> and Clara Rivera<sup>5</sup>

**Abstract.** New regional seismological data acquired in Colombia during 1993 to 1996 and tectonic field data from the Eastern Cordillera (EC) permit a reexamination of the complex geodynamics of northwestern South America. The effect of the accretion of the Baudó-Panama oceanic arc, which began 12 Myr ago, is highlighted in connection with mountain building in the EC. The Isthmina and Ibagué faults in the south and the Santa Marta-Bucaramanga fault to the northeast limit an E-SE moving continental wedge. Progressive indentation of the wedge is absorbed along reverse faults located in the foothills of the Cordilleras (northward of 5°N) and transpressive deformation in the Santander Massif. Crustal seismicity in Colombia is accurately correlated with active faults showing neotectonic morphological evidences. Intermediate seismicity allows to identify a N-NE trending subduction segment beneath the EC, which plunges toward the E-SE. This subduction is interpreted as a remnant of the paleo-Caribbean plateau (PCP) as suggested by geological and tomographic profiles. The PCP shows a low-angle subduction northward of 5.2°N and is limited southward by a major E-W transpressive shear zone. Normal oceanic subduction of the Nazca plate (NP) ends abruptly at the southern limit of the Baudó Range. Northward, the NP subducts beneath the Chocó block, overlapping the southern part of the PCP. Cenozoic shortening in the EC estimated from a balanced section is ~120 km. Stress analysis of fault slip data in the EC (northward of 4°N), indicates an ~E-SE orientation of  $\sigma_1$  in agreement with the PCP subduction direction. Northward, near Bucaramanga, two stress solutions were observed: (1) a late Andean N80°E compression and (2) an early Andean NW-SE compression.

### 1. Introduction

The Andes of Colombia, Venezuela, and Ecuador represent the northern termination of the Andean belt, which extends for

<sup>1</sup>UMR 5573, Laboratoire de Géophysique, Tectonique et Sédimentologie, CNRS, Université Montpellier II, Montpellier, France.

<sup>2</sup>Departamento de Ingeniería Civil, Facultad de Ingeniería, Universidad de Los Andes, Bogotá.

<sup>3</sup>Seismological Laboratory, California Institute of Technology, Pasadena.

<sup>4</sup>Institut de Physique du Globe, Université Louis Pasteur, Strasbourg, France.

<sup>5</sup>Instituto de Investigaciones en Geociencias, Minería y Química, Bogotá.

<sup>6</sup>Vening Meinesz School of Geodynamics, Institute of Earth Sciences, Utrecht University, Netherlands.

Copyright 2000 by the American Geophysical Union.

Paper number 2000TC900004.  
0278-7407/00/2000TC900004\$12.00

more than 9000 km along the western margin of South America [Mégard, 1987]. Intracontinental deformation in the northern Andes results from the complex interaction between three lithospheric plates (Figure 1). The Nazca oceanic plate is converging eastward at 6 cm/yr relative to northwestern South America (NWSA); the Caribbean plate is moving at 1-2 cm/yr to the E-SE relative to NWSA [Freymueller *et al.*, 1993; Kellogg and Vega, 1995].

The Eastern Cordillera (EC) of Colombia is a N-NE trending intracontinental orogenic belt extending for 750 km from the Ecuadorian to the Venezuelan border. It is located in the eastern part of the northern Andes, where it rises abruptly above the lowlands of the South American craton. The medium height of the chain is close to 3000 m (Altiplano Cundiboyacense), with summits reaching 5500 m.

The genesis of the EC has been a matter of long debate, and various deformation models at the lithospheric scale have been proposed for the northern segment:

1. The oceanic subduction type models suggest that the Caribbean plate subducts beneath the EC [e.g., Pennington, 1981]. In this particular model the North Andean block (corresponding to the Andean ranges of Ecuador, Colombia, and Venezuela) is moving toward the NE relative to the South American plate, along a transpressive system of faults following the front of the EC [Pennington, 1981; Freymueller *et al.*, 1993; Kellogg and Vega, 1995]. Other authors have suggested that the Nazca plate (and not the Caribbean) subducts beneath the EC [e.g., van der Hilst and Mann, 1994].

2. The low-angle thrusting models propose that faulting and folding in the cordilleran crust are the consequence of the reactivation of an east vergent detachment along the middle or lower crust [Dengo and Covey, 1993; Cooper *et al.*, 1995]. These models suggest that the gently dipping detachment extends beneath the Middle Magdalena basin and Central Cordillera and branches off from the Nazca subduction zone beneath the Western Cordillera of Colombia (Figure 1 and Plate 1).

3. The intracontinental deformation type models propose that the northern segment of the EC may result from subduction of the continental lithospheric mantle (CLM) beneath the mountain range [Colletta *et al.*, 1990]. In this particular model the direction of continental subduction has not been determined, and two possibilities have been put forward (east or west dipping subduction).

Some of these authors have suggested that the collision between the Panama-Chocó terrane and NWSA, which occurred at about 12 Ma [Duque-Caro, 1990b], caused uplift and shortening in the EC [Dengo and Covey, 1993; Cooper *et al.*, 1995; Kellogg and Vega, 1995].

On the basis of new seismological, tectonic, and tomographic data, we reevaluate the seismotectonics of Colombia and the

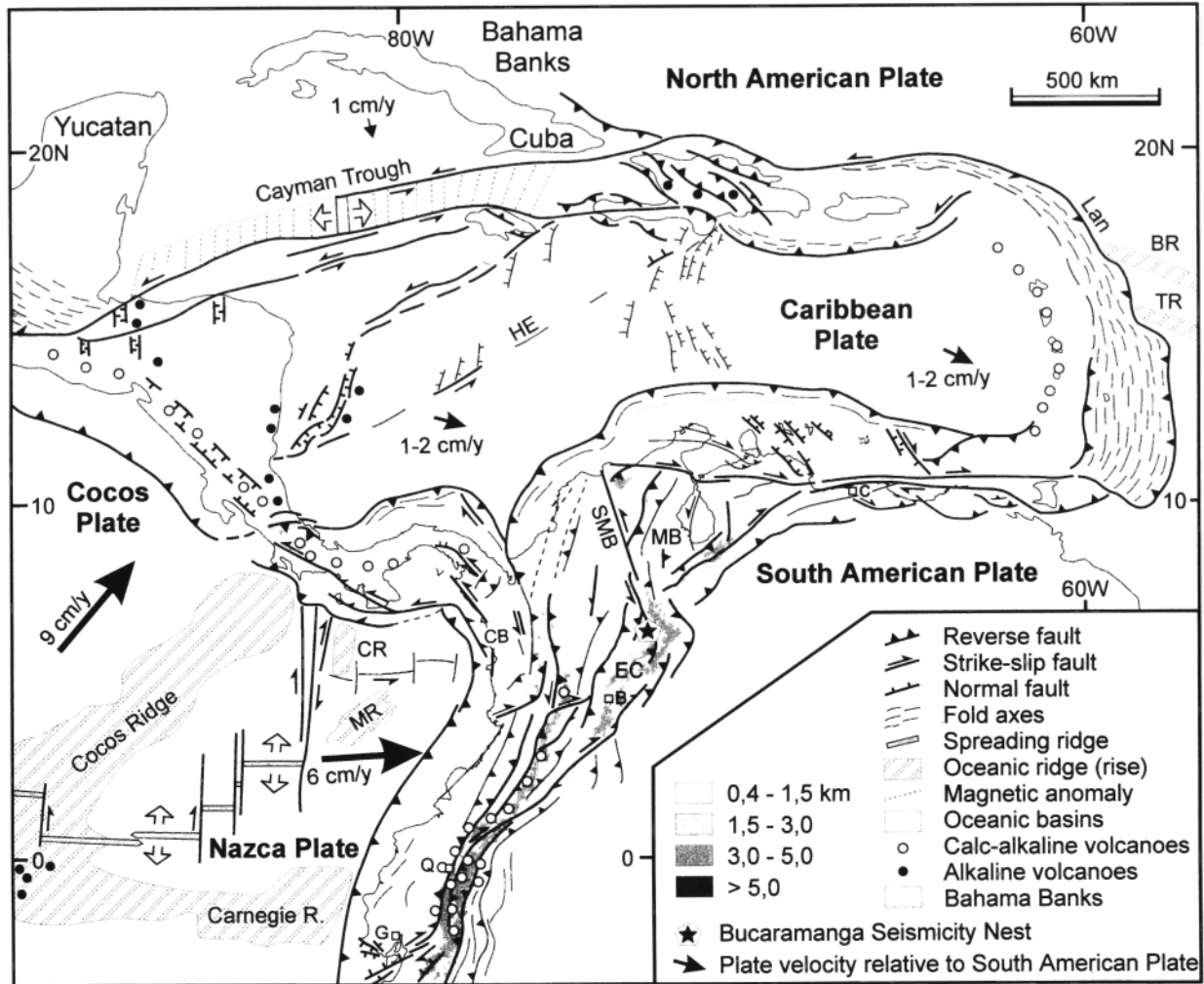


**Figure 1.** Neotectonic plate setting of the northern Andes and the Caribbean region indicating the main active fault systems. The continental deformation in Colombia is the result of the relative motions of the three main plates (Nazca, South American, and Caribbean). Map sources are indicated in Plate 1. G, Guayaquil; Q, Quito; B, Bogotá; C, Caracas; CB, Chocó block; EC, Eastern Cordillera; MB, Maracaibo block; MR, Malpelo Ridge; CR, Coiba Ridge; BR, Barracuda Ridge; TR, Tiburón Rise; HE, Hess Escarpment; SMB, Santa Marta-Bucaramanga fault; Lan, Lesser Antilles Arc.

geometry of subduction zones beneath NWSA. This paper examines the tectonic structure of the northern segment of the EC (which extends from the south of Tunja to Bucaramanga) and its relationship with intermediate seismicity located beneath the range (Plate 1). Seismological data include relocated events from the National Seismological Network of Colombia, recorded between June 1993 and December 1996. Tectonic data include field observations on structural geology and geomorphology concerning active faulting. Tomographic sections across the northern Andes were obtained from a global model which aims to solve lithospheric-scale structures in the mantle [Bijwaard *et al.*, 1998].

In section 2 we shall summarize and discuss the principal geologic and tectonic features of the northern Andes. Section 3 presents a geodynamic model of the Colombian Andes, based on geologic data and tomographic profiles. Sections 4 and 5 are

devoted to the analysis of the seismicity pattern of Colombia and the seismotectonics of the Eastern Cordillera: several seismological and structural cross sections are presented, as well as a stress field map calculated from microtectonic analysis of fault slip data.

## 2. Tectonic Setting of the Northern Andes and the Caribbean

Intracontinental deformation in the northern Andes is characterized by mountain chains associated with large-scale reverse and strike-slip faults. The direction of ranges is generally N-S to NE-SW, compatible with the convergence directions between plates (Figure 1 and Plate 1). The present deformation pattern is marked by the reactivation of large-scale fault zones, inherited from previous tectonic phases. Eastward movement of

the Nazca plate is partly absorbed along the east dipping subduction zone beneath NWSA and along several continental fault systems that are subparallel to the mountain chains.

### 2.1. The Andes of Ecuador

The Andean chain in Ecuador displays two main ranges roughly parallel to the oceanic trench, separated by the Inter-Andean Depression (located eastward from Quito) (Figure 1). The Western Cordillera of Ecuador is composed of oceanic rocks accreted to the continent along a major suture zone, during late Cretaceous and early Tertiary [e.g., *Aspden and Litherland*, 1992]. The Ecuadorian Inter-Andean Depression corresponds to an allochthonous block characterized by an uppermost Pliocene-Quaternary basin which is located between two N-S trending reverse basement faults [*Lavenue et al.*, 1995]. Reverse faults exhibit opposite thrusting vergence creating a "push down" type compressional basin and are connected southward to a major right-lateral fault which strikes N30°E (located eastward from Guayaquil) (Figure 1) [e.g., *Winter et al.*, 1993]. Right-lateral movement is progressively absorbed along E-NE trending normal faults of the Gulf of Guayaquil pull-apart basin [*Winter et al.*, 1993]. The overall fault geometry resembles an extensional horsetail with a restraining bend corresponding to the Inter-Andean Depression.

The Eastern Cordillera of Ecuador (Cordillera Real) is a metamorphic belt which overthrusts the sub-Andean zone located eastward, along the North Andean Frontal fault [e.g., *Aspden and Litherland*, 1992]. The Cordillera Real is limited by two main reverse faults with opposite vergence. The sub-Andean zone is characterized by a series of eastward verging imbricated slices of sedimentary and volcanic rocks [*Baldock*, 1982].

### 2.2. The Andes of Colombia

The Colombian Andes between latitudes 1°N and 8°N display three main ranges, the Western, Central, and Eastern Cordilleras, which merge southward into a single range (Plate 1). The Western and Central Cordilleras are aligned parallel to the Pacific coast and are separated by the Cauca-Patía Intermontane Depression (CPID). The Eastern Cordillera diverges progressively from the Central Cordillera along a N-NE direction. The Magdalena River flows northward along the wide valley located between these two ranges (Plate 1). The nature and composition of the three Cordilleras are substantially different, each one resulting from distinct tectonic processes that affected NWSA during the Mesozoic and Cenozoic (Table 1).

The Romeral fault system (RFS), which extends along the boundary between the CPID and the Central Cordillera, subdivides the Colombian Andes into two main regions: The "Occidente" and the "Oriente" located west and east of the RFS, respectively. This fault system joins the Ecuadorian suture zone farther south as mentioned in section 2.1.

The evolution and structural style of the "Occidente" has been fashioned by convergence between the proto-Pacific or proto-Caribbean plate and NWSA. Mountain ranges located to the west of the RFS are composed of oceanic rocks accreted to the western margin of South America during the Mesozoic and Cenozoic [e.g., *McCourt et al.*, 1984; *Pindell and Barrett*, 1990; *Restrepo-Pace*, 1992; *Kellogg and Vega*, 1995]. During Cretaceous and early Cenozoic the Farallon plate approached NWSA from the

SW leading to oblique subduction along the old continental margin and to large dextral movements along the RFS [*Grösser*, 1989]. The breakup of the Farallon plate into the Nazca and Cocos plates at 25 Ma reoriented convergence between NWSA and the Farallon / Nazca plate from a NE-SW to an E-W direction [*Lonsdale and Klitgord*, 1978; *Pilger*, 1983]. Convergence has remained approximately E-W until present, leading to transpressive deformation along continental faults trending N-NE in southwestern Colombia. The Serranía del Baudó is a narrow range located to the west of the Western Cordillera. It is an exotic piece of Central America, which was part of an island arc that extended toward Panama (Figure 2). The island arc was linked to subduction of the Pacific plate beneath the southwestern margin of the proto-Caribbean plate [e.g., *Wadge and Burke*, 1983]. The eastward movement of the Caribbean plate with respect to NWSA during early and middle Miocene was partly absorbed by subduction of oceanic lithosphere beneath the northwestern corner of South America [*Pindell and Barrett*, 1990]. Subduction led to the closure of the oceanic domain located in between the Baudó-Panama island arc and the Western Cordillera. This oceanic domain corresponded to the southern part of the paleo-Caribbean plate, and it was separated from the Nazca plate by an approximately east-west trending transform fault (Figure 2a). Finally, collision between the exotic block and NWSA occurred toward Middle Miocene time (12 Ma) [*Duque-Caro*, 1990b]: the eastern part of the island arc (including the Baudó range and northeastern Panama), known as the Chocó block (CB), was accreted to the northwestern flank of the Western Cordillera. The collision between the western Panama island arc and South America occurred later, mainly during late Miocene and Pliocene [*Mann and Corrigan*, 1990]. The final closure of the Pacific-Caribbean gateway occurred during the late Pliocene. *Duque-Caro* [1990a] proposes that the Panamanian isthmus became completely emergent between 3.7 and 3.1 Ma, whereas *Keller et al.* [1989] estimate that the closure of the isthmus began at 2.4 Ma, with final closure at 1.8 Ma.

The CB is limited by active fault systems such as the Uramita fault zone (UFZ) to the east and the Istmina deformed zone (IDZ) to the south (Plate 1) [*Duque-Caro*, 1990b; *INGEOMINAS*, 1997]. The IDZ is characterized by transpressive right-lateral faults trending E-NE, such as the Garrapatas fault (GAF), which shows neotectonic activity [*París and Romero*, 1994; *Guzmán et al.*, 1998]. The UFZ is conjugate, trending to the N-NW and exhibiting a transpressive left-lateral movement. The accretion of the CB is contemporary with the onset of the major "Andean" tectonic phase in the EC, which began at 10.5 Ma and continued during Plio-Quaternary time [e.g., *Cooper et al.*, 1995; *Kellogg and Vega*, 1995; *Taboada et al.*, 1998].

Late Tertiary and present deformation along the RFS is characterized by east dipping reverse and strike-slip faults which are part of a larger west vergent, basement-involved fold and thrust belt [*Alfonso et al.*, 1994; *París and Romero*, 1994; *Guzmán et al.*, 1998]. The RFS trends N-NE and shows a right-lateral component in southwestern Colombia (Plate 1). Northward of latitude 4°N it shows a left-lateral component which is probably associated with E-SE convergence between the Chocó block and NWSA. The Armenia 1999 earthquake, earthquake 13 in Table 2, clearly illustrates the left-lateral movement along the RFS: the focal mechanism obtained from the



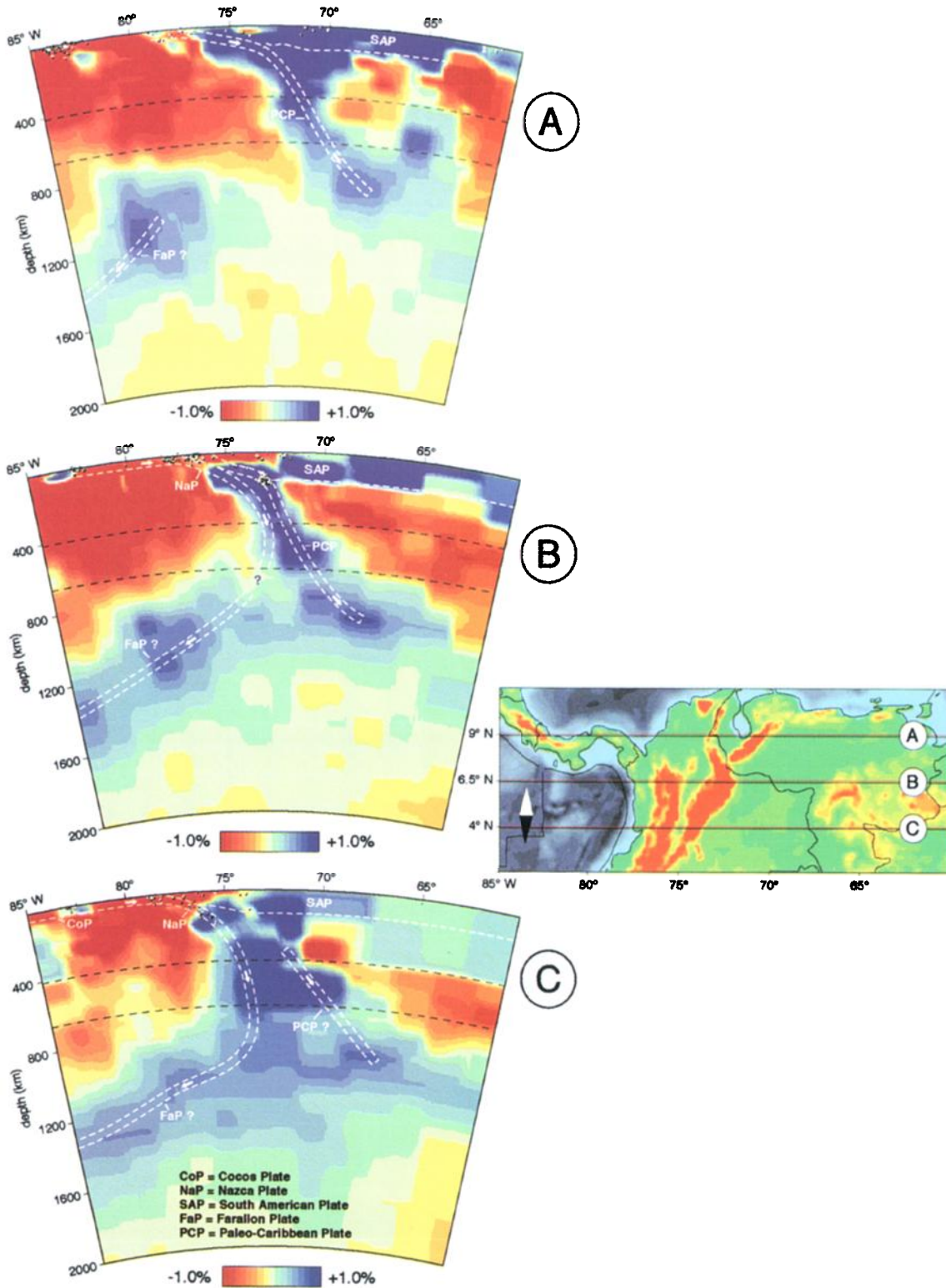


**Plate 2.** Tomographic sections across the northern Andes and hypothetical interpretations in terms of subduction of oceanic lithospheres.

Table 1. Age and Origin of the Main Ranges and Cordilleras in Colombia

Mountain Chain	Composition	Neogene Orogenic Phases
Baudó-Panama Ranges	The Baudó-Panama ranges consist of several exotic blocks, which were part of an oceanic island arc located along the western margin of the proto-Caribbean plate.	The collision between the eastern part of the island arc and NWSA occurred during the middle Miocene at 12 Ma (Chocó block). The collision between the western Panama island arc and South America occurred mainly during late Miocene and Pliocene.
Western Cordillera	The WC is composed of oceanic rocks (turbiditic deposits and ophiolites) accreted to the western margin of South America during the Mesozoic and early Cenozoic.	The WC is characterized by a late Cenozoic thrust and fold belt linked to the Nazca subduction (south of 5°N) and to the accretion of exotic Caribbean blocks (north of 5°N). Neotectonic deformation is observed along both foothills.
Central Cordillera	The CC is composed of a pre-Mesozoic, polymetamorphic basement including oceanic and continental rocks, intruded by several Mesozoic and Cenozoic plutons related to subduction. Active volcanoes linked to the Nazca subduction zone are located along the crest of the Cordillera (south of 5°N).	The CC is limited by reverse fault systems located along the foothills, which root beneath the range. The Romeral fault, located along the western flank, has been activated since Oligocene, combining strike-slip and reverse movement: Neogene transpressive movement is right lateral in southwestern Colombia, and left lateral northward of 4°N.
Eastern Cordillera	The EC is composed of a Precambrian and Paleozoic polymetamorphic basement, deformed during several pre-Mesozoic orogenic events. Basement rocks are covered by a thick sequence of Mesozoic and Cenozoic sedimentary rocks, strongly deformed during Neogene by thrusting and folding.	The Andean tectonic phase began at 10.5 Ma and continued during Plio-Quaternary time. Incipient transpressive deformation in the flanks occurred during the Paleogene. Intracontinental deformation in the northern EC is closely related to accretion/collision episodes along the active margin of NWSA and to shallow subduction of the PCP beneath the Cordilleras (north of 5.2°N).

NWSA, northwestern South America; WC, Western Cordillera; CC, Central Cordillera; EC, Eastern Cordillera; PCP, paleo-Caribbean plateau.

Harvard centroid moment tensor (CMT) file is coherent with a left-lateral N-NE active fault observed in the field (the strike, dip, and rake of the focal planes are 8°/65°/-21° and 107°/71°/-153°, respectively). This result is coherent with the convergence direction between Panama and Bogotá determined by Global Positioning System (GPS) measurements [Kellogg and Vega, 1995]. Quaternary tectonic activity in the RFS is moderate to high, as shown by shallow seismicity and neotectonic geomorphologic features observed along the western flank of the Central Cordillera up to latitude 8°N (Nazca plate influence zone) [París and Romero, 1994]. The RFS is generally assumed to extend northward between latitudes 8°N and 11°N across the Colombian Caribbean region for more than 300 km in a N-NE direction (Plate 1). Nevertheless, fault traces are less visible at the surface in this area, and neotectonic activity is very low. The paleosuture subdivides the Caribbean region into two principal domains [Duque-Caro, 1984]: (1) a continental domain located eastward of the RFS, characterized by Paleozoic and Mesozoic basement rocks, and (2) an oceanic domain west of the fault, characterized by basement and sedimentary rocks of oceanic affinity. A thick sedimentary cover of Tertiary marine sediments and Quaternary fluvial and lacustrine deposits overlies the continental rocks. Quaternary sediments are located within the lowlands corresponding to the Lower Magdalena and Lower Cauca floodplains.

The most important tectonic structures observed to the west of the RFS in the Caribbean margin are the San Jacinto and Sinú thrust and fold belts composed of deformed oceanic rocks [e.g., Case et al., 1984]. The Sinú – San Jacinto terranes resulted from two progressive accretionary episodes of deformation and emergence, during the early Cenozoic (San Jacinto belt) and late

Cenozoic (Sinú belt) [Duque-Caro, 1984]. The San Jacinto belt is characterized by three moderate ridges, which extend northward for 360 km along a discontinuous range. The thick sedimentary sequence observed in the area consists of upper Cretaceous and lower Tertiary deep-sea rocks, deformed by compressive tectonics [Duque-Caro, 1984]. Large-scale anticlines and thrust faults trending N-NE and with vergence toward the Caribbean sea have been described. These structures are mostly linked to convergence between the Caribbean plate and NWSA. The eastern flank of the thrust belt is covered with Quaternary fluvio-lacustrine deposits.

The Sinú thrust belt is located between the Sinú fault to the east and the South Caribbean Marginal fault to the west (Plate 1). This younger belt extends parallel to the Colombian Caribbean margin along more than 500 km. It comprises several anticlines located inland and progressively continues offshore along the continental shelf and the inner slope of the active Caribbean margin [e.g., INGEOMINAS, 1997]. The deformation pattern is similar to the San Jacinto thrust belt and displays west vergence fault-bend folds within a thick cover of Neogene sediments [Duque-Caro, 1984]. The internal structure of these belts is compatible with a low-angle basal friction accretionary prism. Active folding along the toe of the prism has been interpreted in terms of low-angle subduction of the Caribbean plate beneath northwestern Colombia [Toto and Kellogg, 1992].

The Colombian "Oriente" consists of the Central and Eastern Cordilleras, which lie at or near the western margin of the Precambrian Guyana shield. Rocks observed in these mountain ranges have experienced several phases of tectonic deformation as a result of plate motion since the breakup of Pangea [e.g., Mégard, 1987].

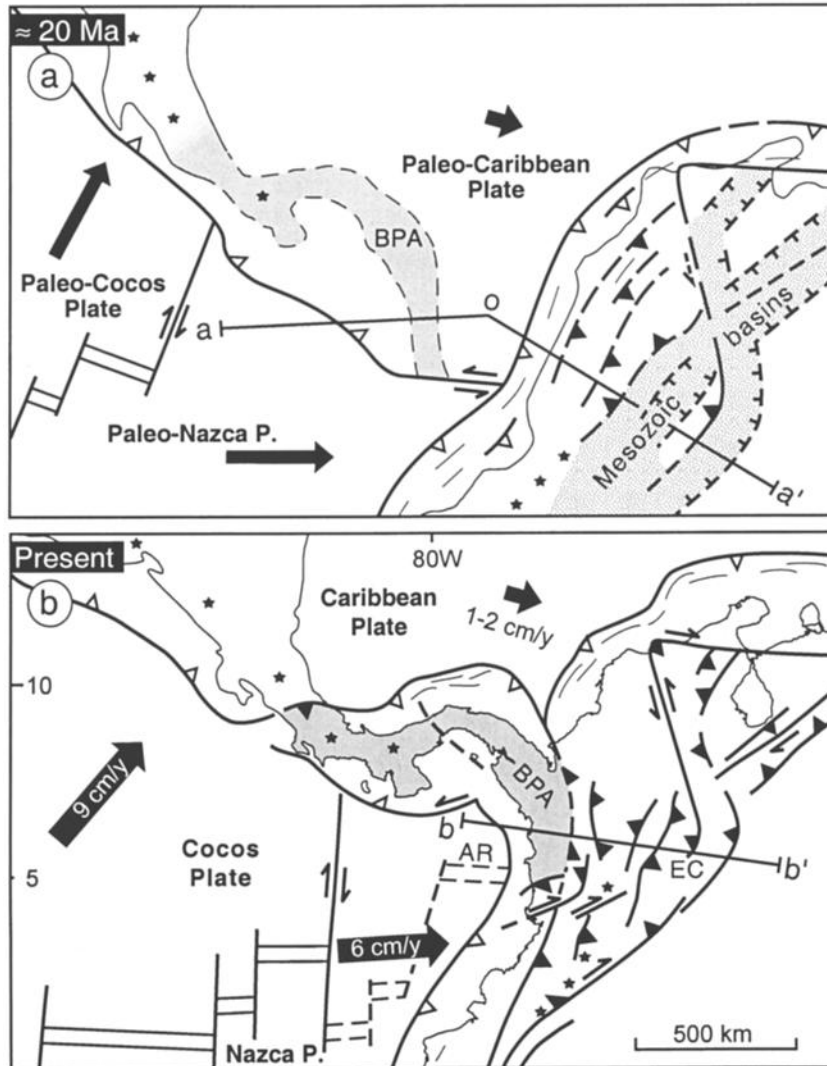


**Figure 2.** Schematic tectonic reconstructions of the northern Andes and the Caribbean (a) at 20 Ma and (b) at present time. Reconstructions illustrate the geodynamic pattern before and after the collision of the Baudó-Panama island arc (BPA; dark shaded area), which began at 12 Ma. Stars indicate approximate location of active volcanism; cross sections a-a' and b-b' are illustrated in Figure 3. EC, Eastern Cordillera; AR, Abandoned Ridge.

The Central Cordillera (CC) is composed of a pre-Mesozoic, polymetamorphic basement corresponding mainly to a disrupted, medium- to low-pressure, metamorphic belt including rocks of both oceanic and continental character [McCourt *et al.*, 1984]. Basement rocks (largely Paleozoic) are intruded by several Mesozoic and Cenozoic plutons related to the subduction of oceanic lithosphere underneath the Andean chain. Recent magmatic activity is concentrated along the crest of the Central Cordillera, where active volcanoes with summits attaining heights of 5750 m are located.

The western flank of the CC is steeper than the eastern flank and has been uplifted by transpressive movement along faults dipping eastward, which belong to the RFS (for instance, the 1999 Armenia earthquake). The eastern flank of the CC is characterized by west dipping reverse faults located along the foothill of the Magdalena valley. Strike-slip right-lateral faults

trending E-NE cut across the CC and the Magdalena valley between latitudes 4°N and 5°N (e.g., the right-lateral Ibagué fault) [Vergara *et al.*, 1996]. These strike-slip faults are parallel and form an "en echelon" system with the Garrapatas fault zone. Thus they are probably associated with the accretion of the CB (Plate 1).

### 2.3. The Eastern Cordillera

The EC is characterized by a Precambrian and Paleozoic polymetamorphic basement, deformed during several pre-Mesozoic orogenic events. Basement rocks are covered by a thick sequence of Mesozoic and Cenozoic sedimentary rocks, strongly deformed during Neogene time by thrusting and folding [e.g., Irving, 1971]. Jurassic and Cretaceous sedimentary rocks were deposited within large basins whose origin is possibly

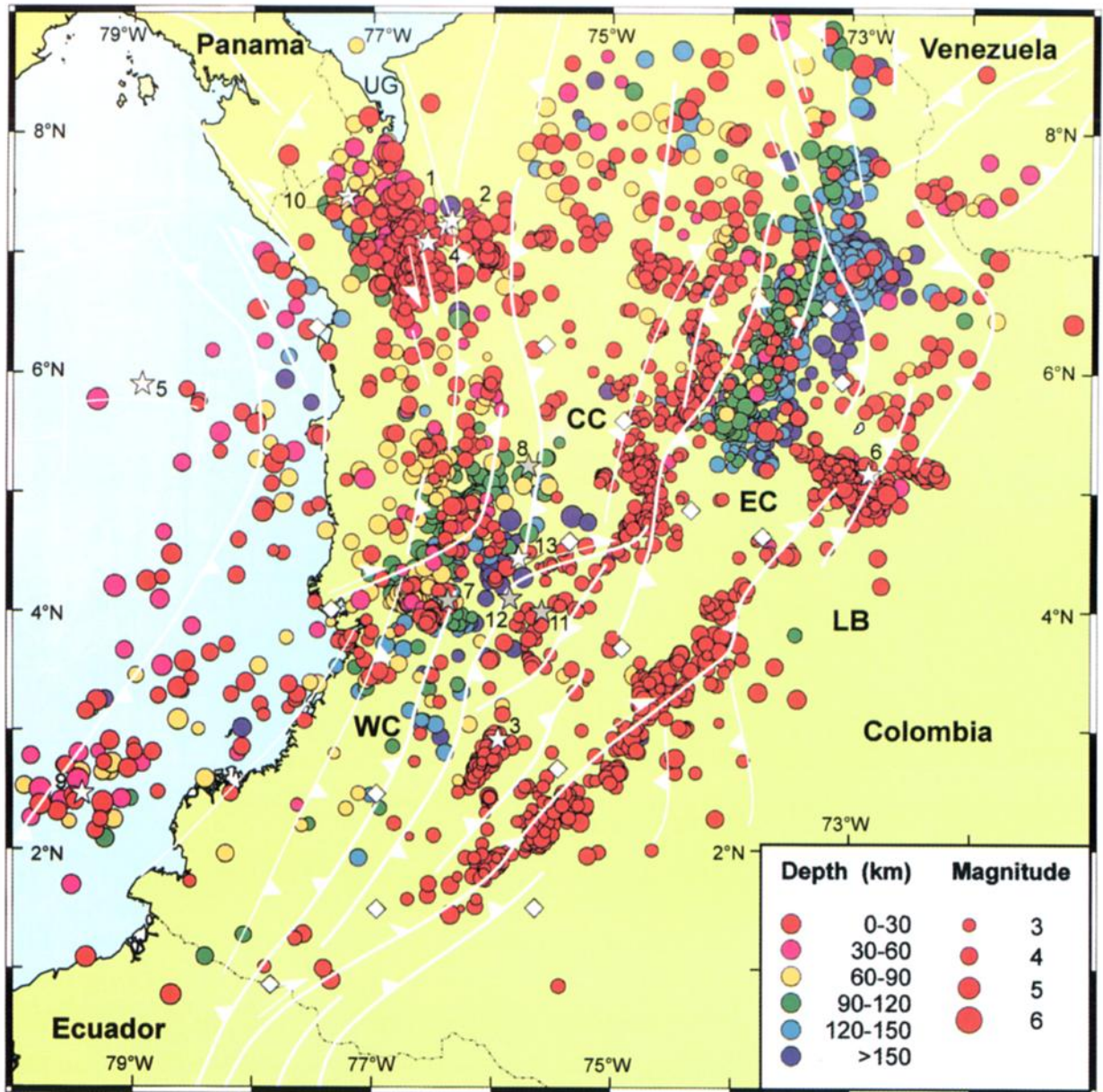
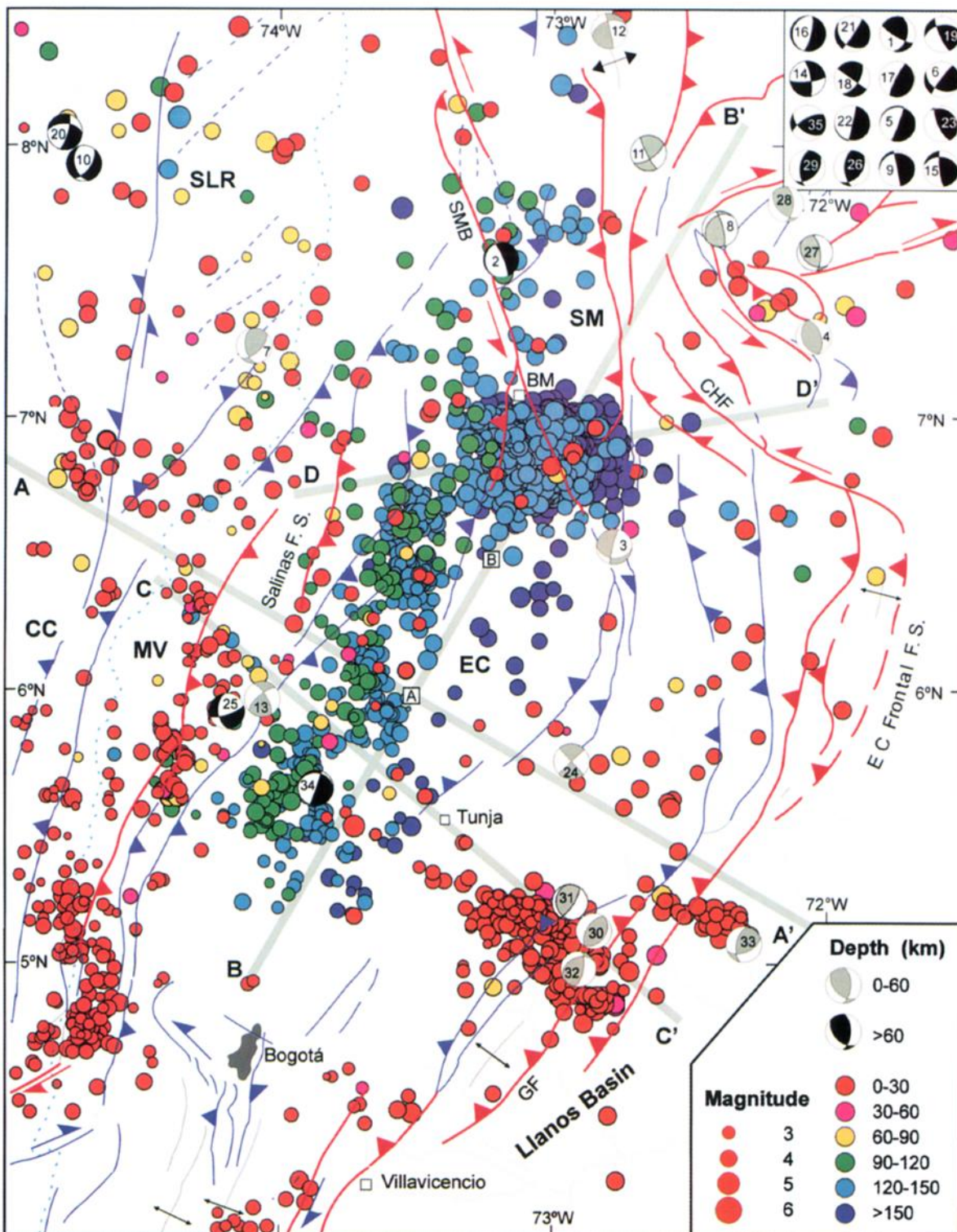


Plate 3. Seismicity of Colombia during the period June 1993 to December 1996, relocated from data of the National Seismological Network of Colombia (NSNC). White diamonds are seismic stations; white and gray stars represent shallow and intermediate strong earthquakes during the last decade, numbered according to Table 2. LB, Llanos basin; UG, Uraba Gulf.



**Plate 4.** Seismicity (June 1993 to December 1996), focal mechanisms, and tectonics of the northern half of the Eastern Cordillera. Orange circles correspond to crustal seismicity; green and blue circles correspond to intermediate seismicity. Active faulting and folding and abbreviations are shown with the same symbols as those in Plate 1. Vertical cross sections A-A' to D-D' of Figure 4 and Plates 4 and 5 are indicated by thick gray lines. The upper right inset shows mechanisms associated with the Bucaramanga nest. Mechanisms correspond to Harvard centroid moment tensor (CMT) solutions from 1976 to 1998.

related to (1) continental rifting since Triassic, as a consequence of an extensional tectonic regime in NWSA, linked to the separation between North America and South America [Mojica *et al.*, 1996], or (2) back arc basin extension located east of the Central Cordillera, as a consequence of subduction of the Farallon oceanic plate beneath NWSA.

Graben systems extended in a N-NE direction, from the Cordillera Real in Ecuador all through the EC of Colombia, the amount of extension increasing northward [e.g., *Etayo et al.*, 1969; *Mojica et al.*, 1996]. The direction of grabens changes to N-NW in the northern end of the EC: namely, it becomes parallel to the Santander Massif (SM). From here the graben system branches into at least three independent basins trending NE: one parallel to the Mérida range, another one at the present location of the Maracaibo lake, and the last along the Perijá range, at the limit between Colombia and Venezuela (Plate 1). These three branches terminate abruptly against the east-west Oca strike-slip fault. Mesozoic basins located south of the Oca fault were formed on thinned continental crust subjected to a mean E-SE trending extension and are oriented accordingly. Other east-west trending Mesozoic grabens have been described north of the Oca fault.

Later on, compressive Cenozoic deformation reactivated some of the normal faults that bounded the Mesozoic basins, inverting their sense of movement [e.g., *Colletta et al.*, 1990, 1997]. The two main inherited fault directions in the EC correspond to NE-SW and N-S trending faults. Tectonic inversion of basement faults created faulting and folding of the thick sedimentary sequences (mostly marine) deposited in the Mesozoic basins.

At least three distinct pre-Andean transpressive deformation phases have been observed in the Magdalena valley and the EC during the Paleogene [e.g., *Cooper et al.*, 1995; *Casero et al.*, 1997]: (1) a Late Cretaceous – early Paleocene deformation phase mostly present in the Upper Magdalena valley and the southern segment of the EC, which was linked to the final accretion of oceanic crustal fragments of the Western Cordillera [McCourt *et al.*, 1984], (2) an early to middle Eocene tectonic phase, which created west vergent thrusting and folding in the Middle Magdalena, and (3) a lowermost Oligocene compressive phase characterized by thrusting and folding along west vergent tear faults in the western flank of the EC [Branquet *et al.*, 1999]. The late Eocene-early Oligocene tectonic phase also created east vergent thrusting along the eastern foothill of the EC [e.g., *Corredor*, 1997]. During these phases, transpressive right-lateral deformation probably occurred along the Romeral and Salinas fault systems as a result of oblique convergence between the paleo-Caribbean plate and NWSA. The accretion of the San Jacinto terrane, which occurred during Paleogene [Duque-Caro, 1984], seems to be well correlated with the Eocene and Oligocene transpressive phases mentioned previously.

The EC widens progressively northward showing different tectonic styles and a varying morphology. The southern segment is a narrow range with moderate relief, not exceeding 2500-3000 m along the mountain crest (Plate 1). Major right-lateral faults trending NE displace basement rocks (e.g., Algeciras - Altamira fault system) [Vergara, 1996]. Reverse faulting is observed in restraining bends and in N-NE trending faults located along the foothills.

The central segment encloses the "Sabana de Bogotá," a high plateau located at 2700 m. Reverse faults dipping toward the range are observed in both foothills (Plate 1). Major uplift in the

Sabana de Bogotá area occurred between 3 and 5 Ma as revealed by palinologic data from Pliocene deposits [Helmens and Van der Hammen, 1995]. However, pre-Pliocene compressive deformation has been identified in the EC from stratigraphic and tectonic analysis. Neogene and, in particular, Miocene compressive deformation is visible in the axial zone of the EC, where folded sedimentary rocks are overlain by tilted Pliocene deposits with a pronounced angular unconformity (e.g., Tunja area [Taboada *et al.*, 1996]).

Compressional deformation and thrusting along "en echelon" reverse faults located in the eastern foothills (Servitá – Santa María (SSM), Guaicáramo (GF), Yopal, and EC Frontal faults) are mainly associated with collision and convergence of the Panama-Baudó island arc located to the west. These faults are known as the Piedemonte Llanero fault system (PLFS) [INGEOMINAS, 1997]. Thrusting along the PLFS also absorbs right-lateral slip along the Algeciras-Altamira fault system in the southern segment. Evidence of active faulting along the PLFS is numerous and includes thrustured Quaternary terraces and fault scarps in young alluvial deposits.

The northern segment of the EC extends from the south of Tunja to Bucaramanga. In this area the width of the range is greater than 200 km, and the highest summits attain 5500 m. The morphology of this segment is characterized by three major NE trending topographic highs which are truncated southward (Tunja area). These highs are separated by two drainage areas, and they are associated with reverse faults which progressively die off toward the SE [Taboada *et al.*, 1996]. This segment is bounded northward by a major left-lateral, strike-slip fault known as the Santa Marta-Bucaramanga (SMB) fault. Strike-slip movement along the SMB fault is absorbed southward by west vergent reverse faults which overthrust the Magdalena valley (Salinas fault system, Plate 1). The SMB fault is also connected to east vergent reverse faults located within the axial zone of the EC. The overall fault geometry evokes a compressive horsetail termination. The total left-lateral displacement along the SMB fault has been estimated to be roughly between 50 km and slightly over 100 km in the northern part, and round figures of 100 km have generally been assumed [e.g., *Tschanz et al.*, 1974; *Laubscher*, 1987; *Boinet et al.*, 1989]. In the southern part the horizontal offset decreases substantially as strike-slip movement is absorbed along thrusts of the EC. Left-lateral movement along the SMB fault may have initiated during the Eocene compressional event and occurred mainly since late Miocene [Boinet *et al.*, 1989]; thus strike-slip movement along the SMB fault is concomitant with thrusting and uplift in the EC.

Thrusts trending NE-SW located in the eastern foothill (PLFS) are bent northward at ~6°N (Plate 1): some segments join progressively N-S trending thrusts of the Santander Massif (SM), while others terminate against NW-SE faults combining reverse and left-lateral movement (Chucarima and Morronegro faults). The SM is a N-NW cordilleran branch (roughly parallel to the SMB fault), which largely exposes Paleozoic and Precambrian basement rocks and deformed Mesozoic sedimentary rocks [INGEOMINAS, 1997]. The morphology of the relief located eastward from and delimited by the SMB fault and its horsetail termination is arcuate and shows a relatively continuous mountain crest. The external part of this elbow-shaped relief is bordered by active thrusts that plunge toward the range.

#### 2.4. The Maracaibo Block and the Caribbean

The Caribbean plate moved eastward relative to the South and North American plates during the Cenozoic [e.g., *Wadge and Burke, 1983; Pindell and Barrett, 1990*]. The North American-Caribbean plate boundary exhibits a total left-lateral displacement of around 1000 km parallel to the Cayman trough pull-apart basin (Figure 1). The study of magnetic anomalies in the oceanic crust formed along the north-south trending mid-Cayman spreading center shows that the trough opened by at least 45-50 Ma. Spreading rates are estimated at 15 and 30 mm/yr since and prior to 26 Ma, respectively [*Rosencrantz et al., 1988*]. The spreading rate decrease at 26 Ma implied a decrease by half in E-NE displacement rate between the Caribbean and North American plates. The slowdown of the Caribbean plate may be correlated with the breakup of the Farallon plate that occurred at 26 Ma, changing the boundary conditions along the western Caribbean margin. Between 43 and 26 Ma, Farallon approached the Caribbean from the W-SW at an average velocity of around 7 cm/yr (convergence direction was subparallel to the Cayman trough) [e.g., *Lonsdale and Klitgord, 1978; Pilger, 1983; Wadge and Burke, 1983; Gordon and Jurdy, 1986*]; after the breakup (between 26 Ma and present) the Cocos - Caribbean convergence was around 8 cm/yr toward the N-NE, while the Nazca - Caribbean convergence was around 5 cm/yr eastward (convergence directions are oblique with respect to the Cayman trough) [*Hey, 1977; Kellogg and Vega, 1995*]. Slight convergence between the North and South American plates during Neogene [e.g., *Ladd, 1977*] may have also contributed to the slowdown of the eastward movement of the Caribbean.

The South American-Caribbean plate boundary consists of a broad zone of transpressive right-lateral deformation [*Stéphan, 1985*]. The deformation mechanism evokes slip partitioning in the southern Caribbean accretionary wedge, caused by oblique convergence: thrusting is located along the low-angle South Caribbean Marginal fault, whereas dextral shearing is absorbed along major transcurrent faults located at the rear of the prism (Oca-Ancón, San Sebastian, and El Pilar faults; Plate 1) [*Beltrán, 1993*]. Internal deformation of the plate, northward of the wedge, is characterized by N-NW trending normal faults that are coherent with relative convergence between the North and South American plates (Figure 1). The NW trending normal faults observed in the wedge are also consistent with oblique convergence. Major right-lateral faults trend E-W and display high angles; they are located near the zone separating continental basement rocks from sedimentary rocks in the accretionary wedge. The convergence component between the Caribbean and NWSA along the E-W trending active margin seems to be much lower than the strike-slip component (Figure 1 and Plate 1).

Continental deformation in northern Colombia and northwestern Venezuela is mostly absorbed along active fault systems located throughout the boundaries of the Maracaibo triangular block (MB). The Venezuelan Andes de Mérida range forms the limit between the MB and the craton and is characterized by transpressive deformation: opposite vergence thrusting along the foothills and right-lateral faulting parallel to the axial zone [*Stéphan, 1985; Soulas, 1986*]. The tectonic structure of the range recalls a crustal-scale flower structure. Average Neogene shortening across the Andes de Mérida is estimated at 60 km, and as suggested by *Colletta et al. [1997]*, it

can be associated with a SE dipping intracontinental subduction beneath the range. The MB is being expelled northeastward relative to stable South America by conjugate movement along the N-NW trending SMB fault and the NE trending Boconó fault [e.g., *Mann and Burke, 1984; Soulas, 1986; Beltrán, 1993*].

The MB is bounded northward by the Oca-Ancón transpressive fault system (OA), where E-W trending right-lateral faults stand out [e.g., *Audemard and Singer, 1996*]. The Sierra Nevada de Santa Marta (SN) is a tetrahedral-shaped range located in the northwestern vertex of the MB, which attains 5840 m. It is composed of Paleozoic and Precambrian continental rocks intruded by Mesozoic and Cenozoic plutons [e.g., *INGEOMINAS, 1997*]. These rocks are similar to those observed southward in the San Lucas Range in accordance with large left-lateral displacement along the SMB fault. The boat prow morphology of the SN massif results from the conjugate strike-slip movement of the OA and SMB faults. The N-NE trending Perijá range is located within the MB, absorbing around 20 km of shortening in the crust along thrusts with dominant vergence toward the NW [e.g., *Kellogg and Bonini, 1982*].

### 3. Neogene Geodynamic Evolution of the Colombian Andes

#### 3.1. Schematic Sections Across the Oceanic Basins and the Cordilleras

The genesis of the Colombian Cordilleras is closely related to the boundary conditions along the active margins located toward the east. Figure 3 shows two schematic cross sections that illustrate the influence of the accretion of the Baudó-Panama arc (BPA), which occurred at 12 Ma (cross sections a-a' and b-b' are located in Figure 2).

Cross section a-a' suggests that at 20 Ma the paleo-Nazca plate subducted obliquely beneath the BPA. The paleo-Nazca subduction is coherent with a Middle Miocene calc-alkalic volcanic pulse that has been identified in western Panama from radiometric dating [*Mann and Corrigan, 1990*]. Subduction of the paleo-Caribbean plate (PCP; which is older and thicker) beneath the Cordilleras is also indicated: the subducting plate dips very gently toward the E-SE. Several geological and geophysical observations favor a low-angle subduction of the PCP beneath the Colombian Cordilleras:

1. The absence of magmatism before the accretion of the BPA northward of the Isthmian deformed zone (IDZ, Plate 1) is coherent with a low-angle subduction. The Cenozoic plutonic episodes northward of the IDZ can be divided into a Paleogene magmatic event and a Neogene (postaccretion) magmatic event [*Aspden et al., 1987*]. Paleogene magmatism mainly occurred during the early Eocene and shows intrusives of intermediate composition located along the western margin of the Western Cordillera (WC) north of 5°N [*INGEOMINAS, 1997*]. This magmatism is also observed in the SN and is probably linked to the initial stages of subduction and accretion of the Caribbean plate beneath the northwestern corner of South America. Kinematic reconstructions of the Caribbean plate show that this subduction was active since the early Cenozoic [*Pindell and Barrett, 1990*]. The extinction of Paleogene magmatism is coherent with low-angle subduction: a thin asthenospheric wedge above the subducting slab prevents magmas from forming over

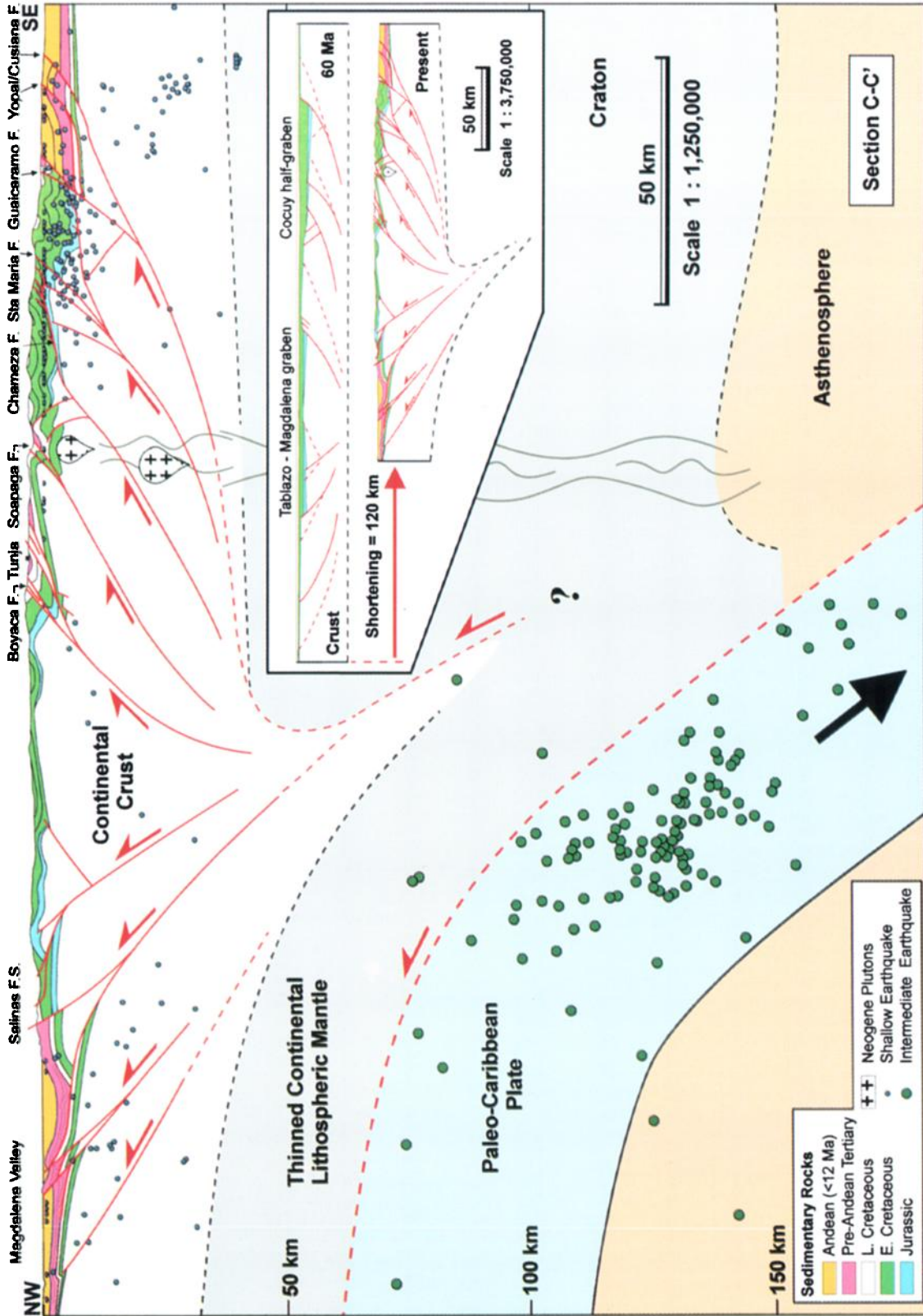


Plate 5. Cross section C-C' orthogonal to the EC through the city of Tunja, including crustal seismicity (Plate 4). Surface tectonics has been obtained by field mapping. The balanced cross sections shown in the inset imply a total Cenozoic shortening of around 120 km.

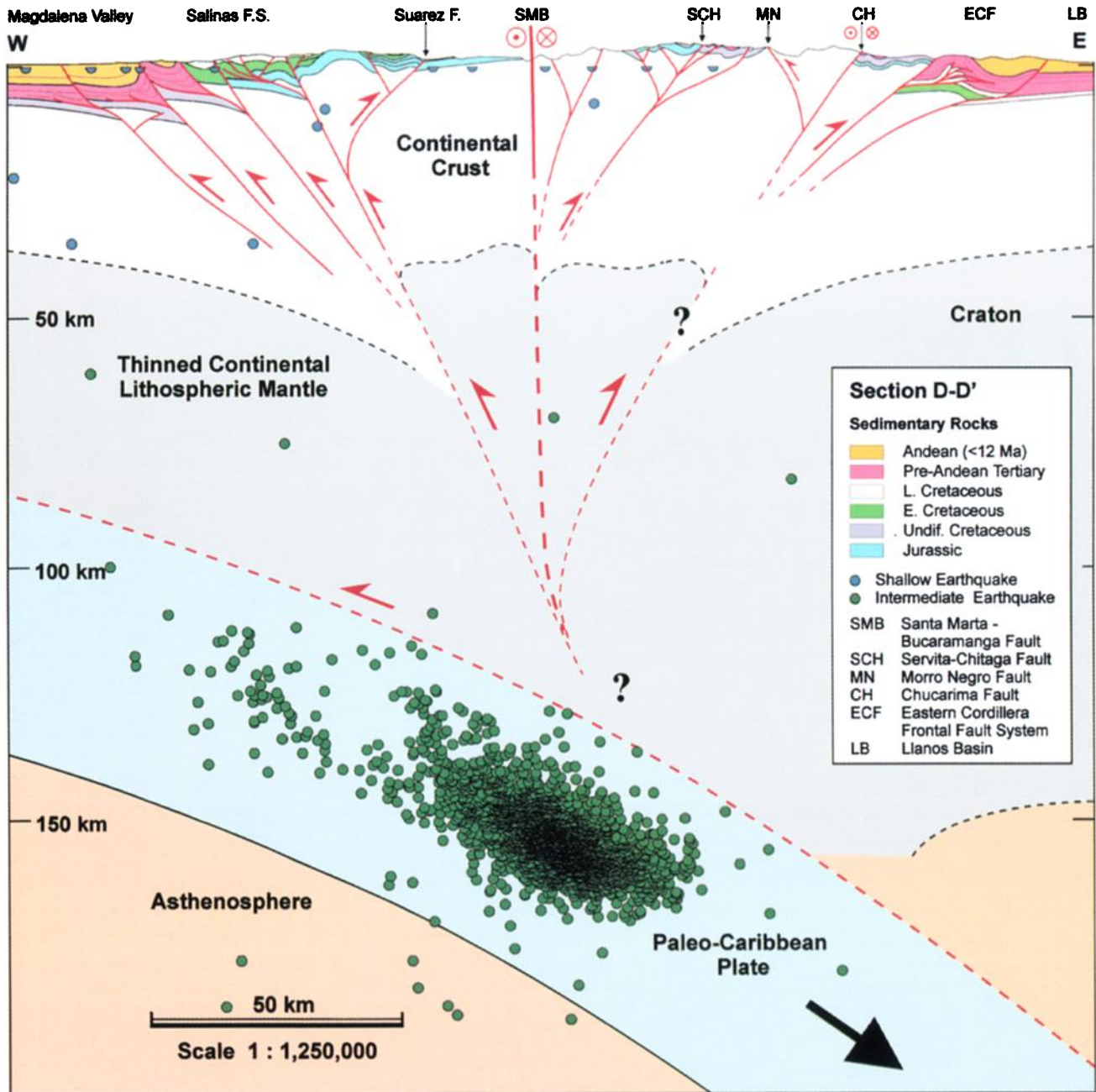
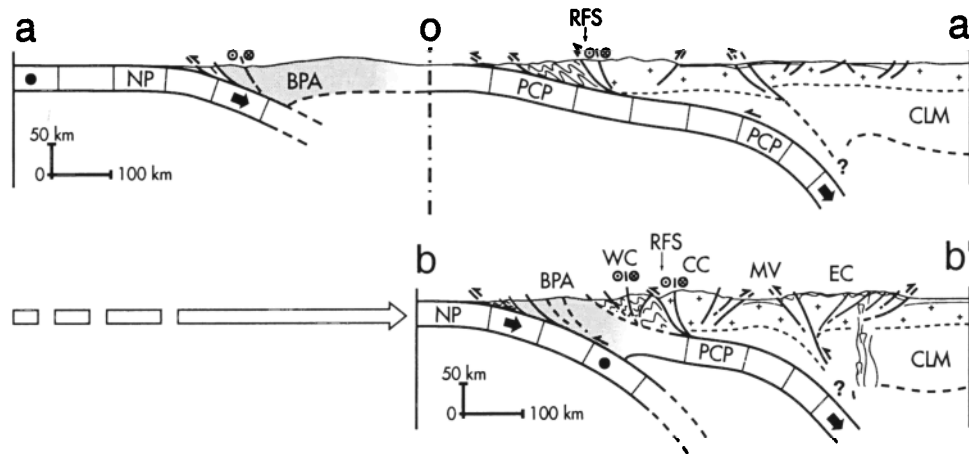


Plate 6. Cross section D-D' passing by the Bucaramanga nest and orthogonal to the SMB fault (Plate 4). Field mapping of active tectonics is included, and its relation to subduction is suggested.



**Figure 3.** Schematic tectonic cross sections of the northern Andes and the Caribbean at 20 Ma (a-a') and at present time (b-b'), illustrating the geodynamic pattern before and after the collision of the BPA, which began at 12 Ma (cross sections are located in Figure 2). Active fault systems in the sections bear arrows and strike-slip symbols. NP, Nazca plate; PCP, paleo-Caribbean plate; RFS, Romeral fault system; CLM, continental lithospheric mantle; WC, Western Cordillera; CC, Central Cordillera; MV, Magdalena valley.

the flat slab region. This assertion has been observed in other regions such as the central Andes, where low-angle subduction is present [Kay, 1999].

2. The age and thickness of the Caribbean plate are also coherent with a low-angle subduction. The Caribbean plate is formed by thick Cretaceous volcanic plateaus separated by deep basins [Mauffret and Leroy, 1997]. Oceanic plateaus and extensive volcanic (basaltic) flows observed in the Caribbean volcanic province were probably formed above the Galapagos hot spot [Mauffret and Leroy, 1997; Sinton et al., 1998]. Thickened oceanic crust causes buoyancy of oceanic plateaus, which is one of the main causes of low-angle subduction [e.g., Gutscher et al., 1999].

3. Present-day low-angle subduction of the Caribbean plate beneath the Maracaibo block has been proposed from scarce seismologic data and tomographic profiles [e.g., Pennington, 1981; Kellogg and Bonini, 1982; Toto and Kellogg, 1992; van der Hilst and Mann, 1994; Malavé and Suárez, 1995; Pérez et al., 1997].

At 20 Ma the continental margin located above the low-angle Caribbean subduction was probably characterized by a thinned continental lithospheric mantle (CLM) (section a-a', Figure 3). Low-angle subduction can result in mechanical thinning and hydration of the continental lithosphere by fluids from the cooling subducting slab [Kay, 1999]. Thus, thinned continental lithosphere is much weaker than normal continental lithosphere is and is particularly susceptible to deformation. The continental margin shows several suture zones and major fault systems. The RFS is represented as a steep fault plunging toward the E-SE. Accreted oceanic terranes of the WC were located beneath the RFS that probably exhibited transpressive movement. At this time, reverse faulting probably occurred along the eastern foothill of the CC, creating a shallow foreland basin eastward [Cooper et al., 1995]. Basins probably extended along the actual Magdalena valley, the EC, and the Mérida Andes (Figure 2a). Early Miocene tectonic activity along the faults that bounded old Mesozoic basins was probably very low.

Cross section b-b' shows schematically the present deformation pattern from the Nazca subduction zone to the craton (Figures 2b and 3). In the section we suggest that the accreted BPA is connected at depth to an east dipping remnant of the PCP. This remnant shows a low angle beneath the CC and the Magdalena valley and becomes steeper beneath the EC. Thus at this latitude the Nazca plate subducts beneath the PCP. The accreted terranes of the Western Cordillera are located in between the BPA and the RFS, which dips steeply eastward. Notice that active faulting in the WC is characterized by subvertical, left-lateral shear zones coherent with E-SE convergence between the Caribbean and NWSA (Figure 1 and Plate 1). The Central and Eastern Cordilleras show active reverse faults along their foothills as described in sections 2.2 and 2.3.

Late Miocene magmatic activity of intermediate composition has been observed near the RFS between latitudes 5°N and 7°N [INGEOMINAS, 1997]. The magmatism is characterized by diorites which have been dated roughly between 12 and 6 Ma [Aspden et al., 1987]. Older magmatic bodies (11 – 12 Ma) seem to be located along the crest of the WC, whereas younger magmatic bodies (6 – 8 Ma) are located along the CPID (Plate 1). The composition of these rocks suggests that they are linked to the subduction of the Nazca plate beneath the accreted terranes of the "Occidente" [e.g., Aspden et al., 1987]. Their emplacement occurred after the beginning of the accretion of the BPA. Partial melting and dehydration of oceanic crust (sediments and eclogites) generally occurs at depths ranging between 90 and 150 km and requires high temperatures existing in the asthenosphere [Wilson, 1989]. We suggest that as the Nazca plate approached the accreted PCP, a wedge of asthenospheric material was located in between them. This wedge favored melting and magmatism during the late Miocene beneath the WC and RFS. Progressive advance of the Nazca plate probably shifted magmatism slightly to the east. Finally, during the Quaternary the subduction shear zone of the Nazca plate was probably located at the base of the BPA and the PCP remnant as indicated in cross section b-b'. The absence of recent volcanic activity associated with the Nazca

subduction zone northward of latitude 5°N may be linked to the presence of the PCP remnant beneath the CC: the oceanic plate may act as a shield that prevents rising magma from percolating through the hanging wall to reach the surface.

In this tectonic model the accretion of the BPA at 12 Ma blocked progressively normal oceanic subduction of the Caribbean plate beneath NWSA. The convergence rate along the suture zone decreased, and active deformation shifted eastward toward weak zones of the continental lithosphere. Shortening localized along Mesozoic extensional basins, creating tectonic inversion of old normal faults [e.g., Colletta *et al.*, 1990]. Notice that thinned and weakened CLM beneath the continental basins favored the shifting of tectonic deformation far to the east. As will be discussed in sections 4.2 and 5.1, shortening of the continental lithosphere is associated with an E-SE dipping subduction of the PCP beneath the EC as indicated in cross section b-b'.

### 3.2. Tomographic Sections Across the Northern Andes

Tomographic sections allow us to study the lithospheric and mantle structures at great depth. In this section we will discuss several tomographic sections performed across the northern Andes from a global model which aims to solve lithospheric-scale structures in the mantle [Bijwaard *et al.*, 1998]. This global model was obtained from an improved inversion of a global earthquake data set, using *P*, *pP*, and *pwP* phases [Bijwaard *et al.*, 1998]. The data set comprises over 82,000 well-constrained earthquakes reprocessed from the International Seismological Centre data set [Engdahl *et al.*, 1998]. The different resolution tests performed beneath northern South America (Venezuela, Colombia, and Ecuador) suggest that the resolution of tomographic results is quite good for the entire mantle. The resolution ranges from 150-km resolution in the uppermost mantle to 250 km near 660-km depth and slowly decreases farther down. Thus lithospheric-scale structures such as oceanic subducting slabs ought to be well described by the model.

Plate 2 illustrates three east-west trending tomographic sections across the northern Andes including seismicity (sections are located at latitudes 9°N, 6.5°N, and 4°N). The hypothetical interpretations of the sections are also given: large high-velocity anomalies indicated in blue are attributed to the subduction of oceanic lithospheric plates composed of colder and denser material.

Cross section A, located at 9°N, suggests a flat subduction of the Caribbean plateau beneath the Maracaibo block. This result is consistent with other tomographic studies which also show a shallow dipping slab in this region [van der Hilst and Mann, 1994]. Eastward, it seems that the PCP plunges at a steep angle (between 50° and 60°) beneath the craton, penetrating into the lower mantle to a depth of around 1000 km. This hypothetical interpretation is coherent with large-scale tectonic reconstructions of the PCP: around 1500 km of the Caribbean plateau have been subducted beneath NWSA since 80 Ma [Pindell and Barrett, 1990]. This implies that there may exist an east-west tear fault in the Caribbean plate along its boundary with NWSA. The surface expression of this limit corresponds to the San Sebastian - El Pilar fault system (Figure 1 and Plate 1). Notice that at this latitude the Nazca subduction, which is located southward, is not visible. Perhaps the high-velocity diffuse zone

located beneath Panama in the lower mantle corresponds to the ancient Farallon-Nazca plate subduction, and it may be correlated with the tomographic sections located southward.

Cross section B, located at 6.5°N, shows an overlap zone where both the Nazca and PCP subductions are present (Figures 2 and 3). As in cross section A, the PCP is interpreted in terms of a shallow subduction beneath the Colombian Cordilleras; eastward, the slab seems to plunge at a steep angle beneath the South American craton, penetrating once again into the lower mantle. The Nazca plate is located westward and is hypothetically interpreted according to another large-scale, high-velocity anomaly that is also visible in cross section C (located at 4°N). The plate seems to plunge at an intermediate angle (close to 35°) into the upper mantle (this assertion is clearly visible in section C, where intermediate earthquakes indicate the dip of the Nazca plate). In the transition zone the dip angle seems to become steeper (nearly vertical). Finally, we suggest that the Nazca plate overturns in the lower mantle and is located along the high-velocity anomaly that dips moderately toward the west. Overturning might occur along a kink located near or below the 660-km discontinuity. Notice that at 4°N the east plunging tendency of the PCP is still visible. This might be an artifact of the model, which cannot resolve the lateral heterogeneity, owing to scarce seismicity. Nevertheless, there may still be a remnant of the PCP at this latitude (indicated with a question mark in cross section C), since the Neogene convergence direction between the PCP and the South American Craton is E-SE.

This hypothetical interpretation should be confirmed by more detailed tomographic studies in NWSA. In sections 4 and 5 we will discuss the relationship between subductions and continental deformation in the northern Andes, according to new seismological and tectonic data from Colombia and, in particular, from the EC.

## 4. Seismicity of Colombia

The National Seismological Network of Colombia (NSNC) consists of 15 short-period stations monitoring the seismicity over the Colombian territory west of the Llanos Basin, operating since June 1993. The accuracy of the seismicity map of Colombia has changed significantly since the installation of this network [Taboada *et al.*, 1998].

### 4.1. Data Analysis

Routine locations made by the NSNC are computed by using the HYPO71 program [Lee and Lahr, 1975], with a velocity model consisting of flat layers for the whole country. Thus lateral variations are not taken into account even though important contrasts exist all over the Colombian territory (mountain ranges and sedimentary and igneous rocks). The only variation allowed in the hypocenter location program is related to the topography, in the form of station corrections.

The database used in this work corresponds to the catalog of seismicity during the period from June 1993 to December 1996. Therefore, in order to reduce location errors and to improve the accuracy of hypocenters, we relocated earthquakes by computing station corrections for sources within a restricted volume. We selected events with at least five *P* and three *S* arrival times in order to establish good station corrections, reduce the probability

**Table 2.** Main Colombian Earthquakes, 1990-2000

Earthquake	Region	Date	Long	Lat	Depth, km	$M_w$
1	Murindó	Oct. 17, 1992	-76. 39°	7. 22°	15. 0	6.6
2	Murindó	Oct. 18, 1992	-76. 34°	7. 27°	15. 0	7.1
3	Páez	June 6, 1994	-75. 94°	2. 93°	15. 0	6.8
4	Murindó	Sept. 13, 1994	-76. 54°	7. 09°	23. 0	6.0
5	Pacific	Sept. 27, 1994	-78. 92°	5. 90°	16. 3	6.1
6	Tauramena	Jan. 19, 1995	-72. 85°	5. 16°	16. 0	6.5
7	S. W. Pereira	Feb. 8, 1995	-76. 36°	4. 09°	68. 2	6.3
8	Intermediate	Aug. 19, 1995	-75. 69°	5. 22°	128. 7	6.5
9	Offshore Tumaco	April 27, 1996	-79. 42°	2. 47°	15. 0	6.1
10	Panama-Colombia	Nov. 4, 1996	-77. 21°	7. 47°	15. 0	6.3
11	Intermediate	Sept. 2, 1997	-75. 57°	4. 00°	213. 2	6.7
12	Intermediate	Dec. 11, 1997	-75. 84°	4. 11°	189.5	6.3
13	Armenia	Jan. 25, 1999	-75. 77°	4. 45°	15. 0	6.1

See Plate 3.

of wrong readings, and obtain well-determined hypocenters. The number of events satisfying the criteria of a minimum of eight arrivals was 6115 for the whole country (Plate 3).

The relocation procedure consisted in choosing events within a volume that was small compared to the distance between the source and the station. Thus any systematic difference between calculated and observed arrival times could be attributed to the deviation of the velocity model with respect to true velocities along the sampled region. The process was iterative because successive locations implied changes in the hypocenter and recalculation of the travel times. The relocation procedure was implemented by the use of the HYPOELLIPSE algorithm [Lahr, 1985], which allows for the relocation of events by using at each iteration new station corrections, obtained from the station delays computed during the previous iteration. The process begins with the definition of the events corresponding to each space window, from the hypocenters obtained by the flat velocity model used by the NSNC. The HYPOELLIPSE program was run with the "Global Option" activated, thus ensuring special attention to the depth range. The relocation volume was chosen to be a running cylindrical window of radius  $0.5^\circ$  and variable depth range ( $0 < h < 30$  km,  $30 < h < 110$  km, and  $h > 110$  km). Afterwards, events were sorted according to their hypocenters, regrouping them into the mobile windows of  $0.5^\circ$  in radius, each  $0.2^\circ$  of latitude or longitude, and the depth ranges described above. The events within each window were processed five times, and at each iteration the averaged time residuals were used as input station delays for the next run. It was observed that after five iterations the residues were converging with a value that was associated with the lateral variations in structure. Some events were repeated since the windows were overlapping. In those cases, the final hypocenter was the average over the common windows for a given event, after verifying that standard deviation in depth was less than 20 km.

The final rms residuals fluctuate around 2 s, which seems to be rather good for the size of the network (1000 km, Plate 3). This value and an estimated precision of 0.2 km/s for the velocity model allow us to conclude that the horizontal error for events inside the network may be less than 5 km and less than 15 km for depth.

#### 4.2. Seismicity and Tectonics

Seismicity patterns resulting from the new NSNC data are much more precise than others previously obtained about Colombia, actually defining the most active zones of the crust along the border of mountain ranges and also showing two main zones of intermediate seismicity under the Central and Eastern Cordilleras. Relocated epicenters from the database are represented in Plate 3 by means of circles (size and color indicate magnitude and depth, respectively). Additionally, the epicenters of the most important Colombian earthquakes since 1992 are indicated with stars (Table 2).

Crustal earthquakes concentrate along the foothills of the Cordilleras and align with the main faults observed at the surface. For instance, seismic activity is clearly associated with the thrusts on each side of the Eastern Cordillera. Notice that several seismic clusters are located around the epicentral zones of major recent earthquakes. The shallow seismicity cluster on the border of the Llanos, located at  $\sim 5^\circ\text{N}$  and  $73^\circ\text{W}$ , is due to aftershocks of the recent 1995 strong earthquakes of Tauramena (earthquake 6 in Table 2). Shallow seismicity is also sharply aligned along the Central Cordillera north of  $2^\circ\text{N}$ . One cluster at  $\sim 3^\circ\text{N}$  and  $76^\circ\text{W}$  is due to the aftershock activity of the Páez earthquake of 1994 (earthquake 3 in Table 2), which produced a large number of huge landslides and distributed damage. It should be observed that the epicentral zone of the recent destructive Armenia earthquake along the Romeral fault system (earthquake 13 in Table 2) was previously quiet, while there was important shallow activity along the neighboring Ibagué strike-slip fault. There is also intense crustal activity along the Western Cordillera north of Buenaventura (BU, on the coast at latitude  $4^\circ\text{N}$ , Plate 1). The shallow cluster located south of the Urabá Gulf (east of the Panama border, Plate 1) is the result of the series of strong earthquakes of Murindó (earthquakes 1, 2, and 4 in Table 2), the largest one of them with magnitude of  $M_w = 7.1$ .

Intermediate seismicity shows a well-defined cluster along the northwestern margin of the Eastern Cordillera. The cluster corresponds to a neat slab running from  $5.2^\circ\text{N}$  to  $7^\circ\text{N}$  in latitude along 150 km, from the north of Bogotá to the Bucaramanga seismicity nest (BSN) (Plates 1 and 3). The activity continues

down to 180 km in depth under the northern segment of the EC; it is roughly oriented N30°E and dips to the E-SE. This elongated cluster corresponds to a well-defined subduction segment, not known before the installation of the NSNC. We suggest that this slab corresponds to a remnant of the PCP, which displays a shallow subduction beneath northwestern Colombia and plunges into the mantle beneath the EC (Figures 2 and 3 and Plate 2). *Pennington* [1981] had suggested an oceanic subduction under this region but on the basis of scarce and poorly defined data and at a larger scale.

The BSN corresponds to a compact and intense concentration of earthquakes located at a depth of ~150 km (at 6.8°N, 73°W) [e.g., *Santo*, 1969; *Dewey*, 1972; *Rivera*, 1989]. Seismicity associated with this subduction changes orientation north of the BSN, trending along a N-S direction. The change in trending direction is especially visible for earthquakes with depths greater than 120 km. This new information shows that the BSN is not an isolated phenomenon as was previously thought. Instead, it is related to an inflection of the subducting surface; more precisely, it is placed at the end of the most active segment of this subduction. The intermediate N-S trending seismicity located northward of the BSN continues northward beneath the Perijá range [e.g., *Malavé and Suárez*, 1995]. Thus it can be interpreted as resulting from a shallow subduction of the Caribbean slab beneath the Maracaibo block (see section 3) [e.g., *Kellogg and Bonini*, 1982].

The cluster of intermediate seismicity observed under the Central and Western Cordilleras at ~3°N to 5.5°N is related to the oceanic subduction of the Nazca plate under South America. The cluster connects to the shallow seismicity observed at the Pacific Ocean off the Colombian coast. The shallow cluster located offshore at ~2.5°N corresponds to the aftershocks of earthquake 9 of Table 2. This event is located within the region affected by the great Colombian earthquake of 1906,  $M_w = 8.8$ , and the large Tumaco 1979 earthquake,  $M_w = 8.2$  [*Kanamori and McNally*, 1982]. Scarce intermediate seismic activity is also observed beneath the WC and CC northward of 5.5°N and southward of 3°N. This seismicity is also attributed to the Nazca subducting slab.

The intermediate seismicity beneath the EC is limited southward, along a roughly east-west trending boundary (with azimuth between N90°E and N100°E), located at 5.2° N. This boundary aligns with the northern termination of the intermediate-seismicity cluster beneath the Western and Central Cordilleras. We suggest that this boundary may correspond to a major E-W transform shear zone. The fault aligns with the southern termination of the Baudó Range and may correspond to the southern limit of the PCP remnant (Figures 2a and 3). Thus its formation is probably linked with shallow subduction of the PCP beneath the Cordilleras and with subsequent accretion and convergence between the Panama-Baudó arc and NWSA. In the eastern part of the shear zone the PCP located northward ought to be in contact with the continental lithospheric mantle (CLM) located southward. Movement in this segment should be right lateral. Notice that the Salinas fault system is located above the shear zone in the continental crust: the trend of the main thrusts changes from roughly N-S southward of the shear zone to N-NE northward of the shear zone (Plate 1). The N-NE trending thrusts are coherent with S-SE convergence between the PCP and

NWSA. The western part of the shear zone may affect the Nazca plate: late Miocene magmatism north of 5°N is slightly shifted westward with respect to recent volcanism in the CC. In this part the shear zone may exhibit left-lateral movement, coherent with active deformation observed in the Colombia – Panama basin (e.g., the Southern Panama fault zone, Plate 1). The shear zone also aligns along the southern margin of the Coiba microplate (Plate 1), where left-lateral movement has been observed from focal mechanisms (e.g., the focal mechanism of earthquake 5 obtained from the Harvard CMT file is coherent with a left-lateral EW fault (Plate 3): the strike, dip, and rake of the focal planes are 7°/69°/-167° and 273°/78°/-21°, respectively). The inversion in the shear sense between the western and eastern part of the shear zone can be explained in terms of the relative velocities of the plates and the lithospheric blocks separated by the shear-zone. Section 5 will present a more detailed analysis of the seismicity of the Eastern Cordillera and its relationship with faulting in the continental lithosphere.

## 5. New Constraints on the Tectonic Structure of the Eastern Cordillera

New seismological and geologic data have been used to study the tectonic structure of the EC at crustal and lithospheric scales. Plate 4 shows the distribution of seismicity around the EC area as a function of depth and magnitude, obtained for the period 1993-1996. Shallow earthquakes indicated in orange are generally located near the foothills of the Eastern and Central Cordilleras, where active and potentially active fault systems are observed. The Salinas fault system, which extends along the western foothill of the EC, is clearly associated with shallow seismicity along imbricated thrusts with vergence toward the Magdalena valley (Plates 1 and 4). The shallow cluster of earthquakes located to the SE of Tunja corresponds to aftershocks of the 1995 Tauramena earthquake. This shallow event reactivated a NE trending reverse fault belonging to the Guacáramo fault system (GF; Plates 1 and 4).

Intermediate seismicity is mostly observed beneath the western flank of the EC and extends northward beneath the Santander Massif (SM). Intermediate earthquake depths along this zone tend to increase toward the E-SE. The intermediate seismic cluster located to the south of Bucaramanga is known as the Bucaramanga seismicity nest (BSN). Intermediate earthquakes in the BSN are located within a prolated volume with azimuth close to E-W, which plunges gently eastward.

Figures 4a and 4b show two cross sections of seismicity, which allow us to analyze the geometry and nature of subduction beneath the EC (the location of the sections is indicated in Plate 4). Cross section A-A' is oriented perpendicularly to the mountain range, and it includes seismicity within a band that covers entirely the subduction zone (the half width of the band is 150 km, measured from the line segment A-A'). This cross section clearly shows a subducting slab that dips ~45°SE, extending between 60- and 200-km depth. This seismicity pattern is interpreted as resulting from active subduction of the PCP beneath the EC (cross section b-b', Figure 3). The flat slab region is located eastward of the Salinas fault system, as indicated by scarce seismicity data. Earthquakes from the BSN are located within the cluster around 150-km depth. Shallow seismicity,

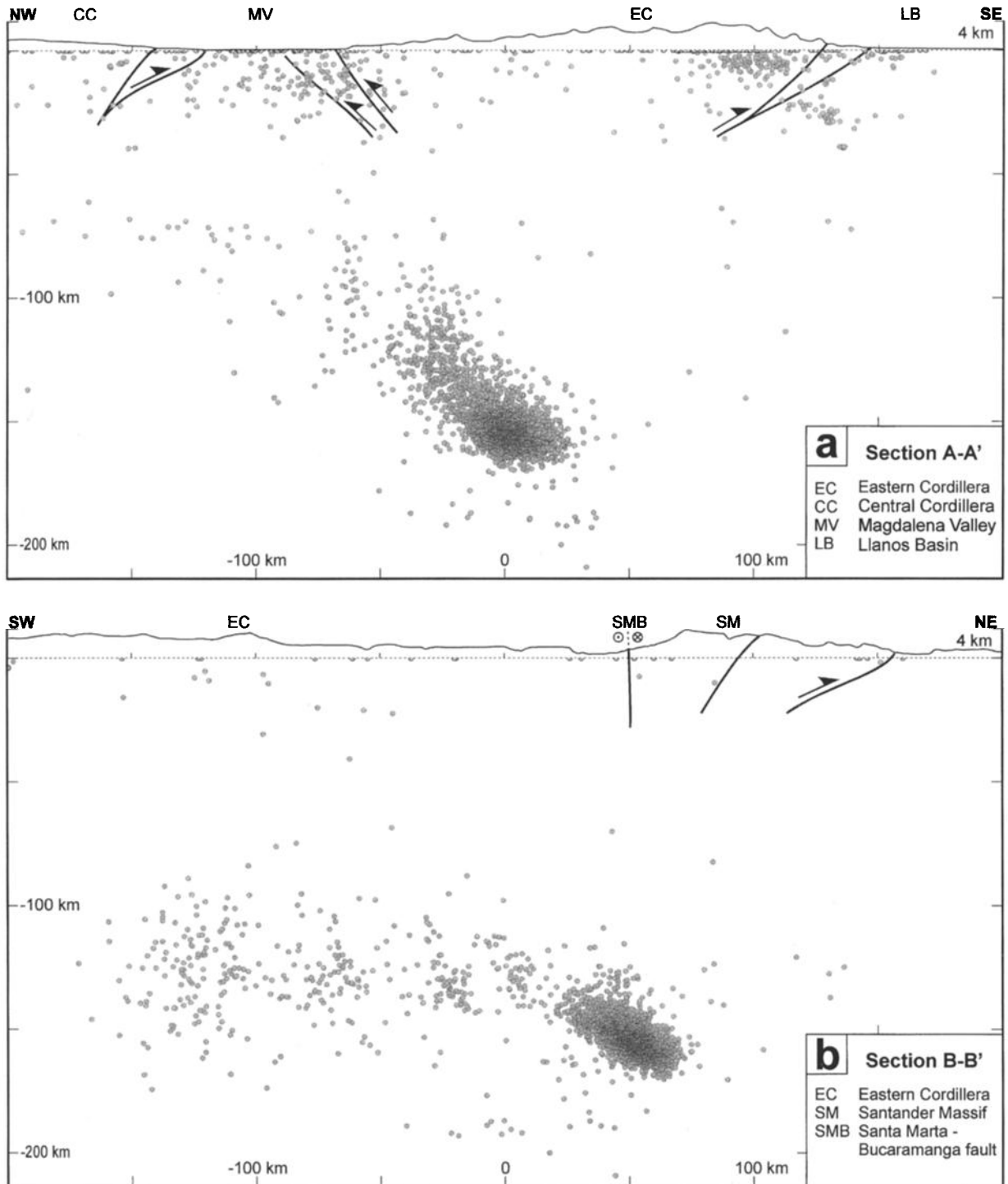


**Figure 4.** Vertical cross sections of seismicity across the Eastern Cordillera (Plate 4) (the vertical exaggeration for the topography is 3). (a) Cross section A-A', orthogonal to the EC and located northward of Tunja. It includes seismicity within a band that covers entirely the subduction zone. (b) Cross section B-B', parallel to the axis of the range. The subduction segment beneath the EC is well separated, with the Bucaramanga nest at the northern end.

corresponding to active faulting in the crust, is concentrated near the foothills of the EC and along the Magdalena valley. Notice the scarce seismicity in the zone lying between the upper crust and the subducting slab. This zone, located between 25- and 60-km depth, is interpreted as the lower crust and a layer of thinned CLM located beneath the Moho (Figure 3). A possible explanation is that the deformation mechanism in these two layers involves mainly ductile shearing. In summary, the deformation mechanism at lithospheric scale involves active subduction and shortening of thinned continental lithosphere beneath the EC.

Cross section B-B' (orthogonal to A-A') oriented along the axis of the EC permits the identification of intermediate-depth seismicity associated with the BSN and separation of this seismicity from that of the remaining part of the subduction (the half width of the band is 40 km, measured from the line segment B-B', Plate 4). The BSN appears as an earthquake cluster located toward the N-NE of the section (beneath the SMB fault).

Focal mechanisms of earthquakes obtained from the Harvard CMT files for the period 1976-1998 are included in Plate 4. The localization, depth, focal planes, magnitude, and date of the Harvard CMT solutions in Plate 4 are available in a supplemental figure (Appendix A).<sup>1</sup> The gray symbols are mechanisms from crustal earthquakes while the black ones correspond to intermediate-depth seismicity. Earthquakes 30, 31, 32, and 33 of the Tauramena sequence, on the eastern foothill of the EC, are in reverse faulting associated with thrusts. Earthquake 7, west of the Magdalena River is also a thrust but is related to the San Lucas range. Earthquakes 4, 8, 27, and 28 belong to the elbow in the SM at the place where it meets the Andes de Mérida range. These earthquakes indicate compression in an E-NE direction, transverse to the trend of faulting along the foothills.

The Bucaramanga nest is represented by 16 focal mechanisms corresponding to events with depths around 150 km (see inset in Plate 4). A preliminary stress tensor obtained from these mechanisms (events between 1977 and 1997) has  $\sigma_2$  oriented NS and  $\sigma_1$  oriented along the EW direction, plunging 30° westward. A previous study made by Rivera [1989] based on polarities of *P* arrivals from the catalog of the International Seismological Centre (ISC) corresponding to the period 1977-1983 provides a stress tensor with  $\sigma_1$  oriented EW,  $\sigma_2$  oriented vertical, and  $\sigma_3$  oriented NS. The inversion of the combined data set shows again  $\sigma_1$  oriented EW, but  $\sigma_2$  is close to  $\sigma_3$  (the stress ellipsoid shape ratio  $R=[\sigma_2-\sigma_3]/[\sigma_1-\sigma_3]$  is near zero), meaning an uniaxial tectonic stress regime. A similar result was already obtained by Rivera when comparing data coming from a local network on top of the Bucaramanga nest with the ISC data from the global network. These different solutions indicate that with the data existing up to now, only an EW oriented  $\sigma_1$  is well constrained, while  $\sigma_2$  and  $\sigma_3$  are free to move on a plane orthogonal to it, and the tectonic stress is in between compressional and strike-slip regimes. The remaining intermediate-depth mechanisms (earthquakes 2, 10, 20, 25, and 34) ought to be located in the PCP and are coherent

with a roughly E-SE trending extensional regime in the subducting slab.

### 5.1. Regional Cross Sections of the Eastern Cordillera

In order to study the tectonic structure of the EC at lithospheric scale, we have reconstructed two regional cross sections by means of geologic data in the upper crust and seismological information (sections C-C' and D-D', Plate 4). Plate 5 illustrates the section across the Tunja area, including seismic activity within a 50-km-width band centered along line segment C-C'.

The tectonic structure in the upper crust was constrained by combining information from several sources: (1) field work in structural geology, neotectonics, and microtectonics in the eastern foothill and the axial zone of the EC; (2) published geologic maps from the Colombian Geological Survey (INGEOMINAS) [e.g., Ulloa *et al.*, 1975, 1976; Renzoni *et al.*, 1983; INGEOMINAS, 1997]; and (3) available information on structural geology and stratigraphy published in the literature [e.g., Colletta *et al.*, 1990; Cooper *et al.*, 1995; Taboada *et al.*, 1996; Vergara *et al.*, 1996; Taboada *et al.*, 1998; Branquet *et al.*, 1999].

As illustrated in Plate 5, the northern segment of the EC results from shortening of thinned continental lithosphere during Cenozoic compressive phases, linked to convergence and subduction of the PCP beneath NWSA. The geometry of the subducting oceanic plate is constrained by earthquake locations: the PCP shows a shallow dip beneath the Magdalena valley, and then it becomes much steeper beneath the EC (attaining 50°-60°). Intermediate-depth seismic activity is concentrated beneath the subduction fault zone and decreases westward toward the Baudó Range (Plate 4). The thinned CLM seems to be affected by a major reverse shear zone with vergence toward the Magdalena valley. Reverse movement along this ductile shear zone can induce mechanical dragging of continental crust down to great depth, as a consequence of shortening of the thinned continental lithosphere. This mechanism has been proposed in other intracontinental collisional belts (Himalayas, western Alps, and Pyrenees) [e.g., Malavieille and Chemenda, 1997]. The crustal tectonic structure and the location of the ductile shear zone are coherent with the east dipping intracontinental deformation model proposed by Colletta *et al.* [1990]; nevertheless, more geophysical studies are necessary to confirm this hypothesis (e.g., gravimetry, tomography, and deep seismic profiles). The thinned CLM is strongly deformed by compression, and it may also be mechanically dragged into the subduction zone by the oceanic plate located beneath (Plate 5). The deformation mechanism in the lower crust and in the CLM beneath the range probably combines pure shear and heterogeneous simple shear. A décollement level may be located along the boundary between the PCP and the thinned CLM.

The total amount of shortening in the EC during the Cenozoic compressional phases is estimated to be roughly around 120 km, according to our balanced cross section. This value is coherent with the estimation proposed by Colletta *et al.* [1990], who calculated at least 105 km of shortening. Nevertheless, shortening could be slightly greater as suggested by several authors: Laubscher [1987] estimated a total compression of ~130 km from Neogene plate kinematic reconstructions; Kellogg and Duque [1994] estimated 140-150 km of late Miocene to recent

<sup>1</sup>Supporting figures (Appendices A and B) are available on diskette or via Anonymous FTP from kosmos.agu.org, directory APEND (Username = anonymous, Password = guest). Diskette may be ordered from American Geophysical Union, 2000 Florida Avenue, N.W., Washington, DC 20009 or by phone at 800-966-2481; \$15.00. Payment must accompany order.

shortening from geological balanced cross sections and geophysical data. The initial crustal structure before shortening corresponded to two large basins where as much as 10 km of sediments accumulated during Mesozoic [e.g., *Etayo et al.*, 1969; *Colletta et al.*, 1990; *Cooper et al.*, 1995]: the Tablazo-Magdalena graben to the NW and the Cocuy half graben to the SE (see inset in Plate 5). These basins were limited by normal listric faults, which rooted into a décollement level in the lower crust. The presence of a thinned and weakened continental lithosphere favored mountain building in this site during Cenozoic. The strength of the crust was diminished by preexisting basement normal faults and by thick Mesozoic sedimentary sequences with low competence.

Tectonic deformation in the northern segment of the EC migrated in space and time during several orogenic pulses, which have been identified by means of detailed stratigraphic analysis [e.g., *Cooper et al.*, 1995; *Casero et al.*, 1997]. As mentioned in sections 2 and 3, shortening occurred as a consequence of varying geodynamic conditions during Cenozoic along the active margins located westward. The deformation mechanism in the crust involves the tectonic inversion of the main normal faults which are often associated with footwall shortcuts [*Cooper et al.*, 1995].

The western margin is characterized by thrusting and folding with vergence toward the Magdalena valley (Salinas and Magdalena valley fault system): at least four main thrusts that cut through the upper crust can be distinguished (each one bears an arrow in the hanging wall indicating thrusting vergence). These faults root at depth into the east dipping ductile shear zone that affects the lithospheric mantle; the total estimated shortening along them is around 45 km. Main thrusts splay in several branches in the upper crust, exhibiting flat and ramp geometries in the sedimentary cover and footwall shortcuts in basement rocks. Flats correspond to décollement levels located along weak sedimentary rocks of the Cretaceous and the early Paleocene (Plate 5). Shortening along west vergent thrusts and folds in the western margin of the EC results from the cumulated effect of the Paleogene and the Andean (post 12 Ma) compressive phases [e.g., *Boinet et al.*, 1989; *Cooper et al.*, 1995]. Paleogene deformation has been established from truncated folds in the Middle Magdalena valley, which are unconformably overlain by late Eocene clastics [e.g., *Morales and Colombian Petroleum Industry*, 1958]. These folds are associated with underlying listric thrusts that probably rooted into the main faults that affected the western border of the Tablazo-Magdalena basin. The Paleogene unconformities are indicated schematically in the pre-Andean Tertiary sedimentary rocks (pink level in the section in Plate 5). Shortening during Paleogene transpressive phases is apparent from the analysis of the tectonic structures: the offset of the Cretaceous in the flat of the Salinas thrust is much greater than the offset of Andean sediments in the frontal ramp (e.g., third thrust from the NW to the SE, Plate 5).

The vergence of thrusting and folding in the axial zone and in the eastern foothill is toward the South American Craton. Nevertheless, back thrusts are also observed in the hanging walls of the major thrusts located along the eastern foothill. Main east vergent thrusts tend to join a low-angle ductile shear zone in the lower crust [*Colletta et al.*, 1990]. In our interpretation this décollement branches off from the shear zone, near the Moho.

The axial zone is characterized by three main reverse faults: (1) the Boyacá fault, which reactivates the normal fault that limited the Tablazo-Magdalena graben [e.g., *Colletta et al.*, 1990; *Taboada et al.*, 1996]; (2) the Soapaga fault, which is less steep and probably corresponds to an old Paleozoic crustal fault reactivated during subsequent tectonic events (P. Cobbold, personal communication, 1995); and (3) the Chámeza fault, which probably reactivates a Mesozoic normal fault that affected the Cocuy half graben. The Chámeza fault joins a low-angle décollement level located at the base of the Early Cretaceous sequence. Movement along the décollement is accommodated by imbricated thrusts with vergence toward the SE (Y. Branquet, personal communication, 1999). Total shortening in this zone is around 40 km and is mainly associated with the Andean tectonic phase.

The eastern foothill is characterized by four main fault systems with vergence toward the craton: the Santa María, Guaicáramo, Yopal, and Cusiana thrusts. The Guaicáramo fault reactivates the main normal fault that limited the eastern border of the Cocuy half graben [e.g., *Cooper et al.*, 1995]. We estimate shortening in the eastern foothill at ~35 km, which occurred mainly during the Andean tectonic phase. The total amount of shortening which we obtained during the Andean phase is roughly between 80 and 100 km; this value is slightly greater than the 68-km estimation proposed by *Cooper et al.* [1995] for the Andean tectonic phase.

Another geologic feature is the existence of small plutons of K/Rb rich rhyolites eastward of the Tunja area, which constitute the sole Tertiary volcanic rocks known in the EC [*INGEOMINAS*, 1997]. The petrographic analysis of these Miocene rocks suggest that their original composition was slightly less acid (rhyodacite, dacite, or trachyte domain) and that they suffered subsequent alteration in the crust by hydrothermalism [*Martinez*, 1989]. We suggest that these rocks may be linked to partial melting associated with subduction of the PCP beneath the EC (Plate 5), yet their precise origin remains uncertain.

Plate 6 illustrates the section across the Bucaramanga nest area including seismic activity within a 50-km band centered along the line segment D-D' (Plate 4). The tectonic structure in the upper crust was constrained combining information from several sources: (1) field work in structural geology, neotectonics, and microtectonics in the northern termination of the EC and in the SM; (2) published geologic maps from the Colombian Geological Survey (INGEOMINAS) [e.g., *Ward et al.*, 1969, 1977; *INGEOMINAS*, 1997]; and (3) available information on structural geology and stratigraphy published in the literature [e.g., *Julivert*, 1958; *Kammer*, 1993; *Corredor*, 1997; *Steuer et al.*, 1997].

Mountain building in this area resulted, as in the whole EC, from Cenozoic shortening of thinned and weakened continental lithosphere. The geometry of the subducting oceanic plate is constrained by earthquake locations: the PCP shows a shallow dip beneath the Magdalena valley (around 15°), and it becomes progressively steeper beneath the EC (attaining 30°-40°). Intermediate-depth seismic activity is concentrated in the BSN, which corresponds to the cluster shown in cross section D-D'. The overall tectonic structure of the chain resembles a lithospheric-scale flower structure. It is characterized by strike-

slip faulting along steep (vertical) faults located in the axial zone and by reverse faulting along thrusts located near the foothills. The Santa Marta - Bucaramanga (SMB) fault is the major strike-slip fault located in between the Santander Massif (SM) and the EC; the fault trace is linear along 700 km except for a compressional jog at latitude 8°N. It shows mainly left-lateral movement along its trace during the Neogene [e.g., Irving, 1971; Tschanz et al., 1974; Boinet et al., 1989]. The section suggests that the SMB fault is subvertical and affects the whole continental lithosphere. The thinned CLM might also be affected by two, steep, ductile shear zones with opposite vergence located beneath the EC and the SM, respectively. These ductile shear zones ought to exhibit transpressive movement, and they join progressively the SMB fault at depth. Reverse movement along them can induce dragging of continental crust down to great depth. Nevertheless, the existence of these shear zones is hypothetical and should be confirmed by other geophysical studies. An alternate interpretation, in particular, beneath the SM, would consist in supposing that crustal reverse faults root at depth into a gently dipping décollement level in the lower crust (and not into a steep ductile shear zone in the lithospheric mantle). In this case, deformation in the crust would be decoupled from deformation in the lithospheric mantle. As in cross section C-C', a décollement level may be located along the boundary between the PCP and the thinned CLM.

West of the SMB fault, the upper crustal tectonic structure is characterized by west vergence reverse faults located along the western flank of the cordillera (Salinas fault system): the fault geometry corresponds to imbricated thrusts that root into the basement. These faults root at depth into the east dipping shear zone that affects the CLM. Splay faults are observed in the Mesozoic and Cenozoic sedimentary cover. As in cross section C-C', Paleogene unconformities are indicated schematically in the pre-Andean Tertiary sedimentary rocks located in both foothills (pink level in Plate 6). Notice the presence of an active back thrust (Suárez fault) which joins at depth the thrusts of the Salinas fault system. These thrusts join northward the trace of the SMB fault (Plate 1). The average altitude of the chain between the Magdalena valley and the SMB fault is around 1500 m.

The upper crustal tectonic structure of the Santander Massif (eastward of the SMB fault) is mainly characterized by east vergent reverse faults. Steep faults such as the Chucarima show a left-lateral component, while shallower dipping faults such as the Frontal fault system show a dominant reverse movement (Plates 1 and 6). This observation suggests strain partitioning in the crust. In the eastern foothills geomorphologic evidences such as uplifted and tilted terraces, pressure ridges, and fault scarps indicate active thrusting along the EC Frontal fault system. The average altitude of the mountain chain between the SMB fault and the Llanos Basin is around 3000 m.

## 5.2. Tectonic Stress Field in the Eastern Cordillera

In order to analyze the neotectonic stress field in the EC, we studied the brittle deformation of sedimentary rocks and Quaternary deposits observed in the axial zone and the foothills. Forty-two different outcrops were studied in detail, where rocks exhibited brittle deformation in relation with mountain building. In these outcrops, microtectonic structures such as striated faults, tension gashes, folds, and stylolites were measured. The

analysis of structural data by means of numerical and graphical methods [Etchecopar et al., 1981; Taboada et al., 1991; Ritz and Taboada, 1993; Taboada, 1993] allowed us to determine the principal stress directions and to establish a new neotectonic stress map at a regional scale (Figure 5). Table 3 summarizes the results obtained from the stress analysis, indicating the number and location of the outcrop, the lithology and age of the rocks, and the orientation of the bedding plane. Stress results include the azimuth and the plunge of the three principal stress axes  $\sigma_1$ ,  $\sigma_2$ , and  $\sigma_3$ , which correspond to the principal compressional, intermediate, and extensional axes, respectively. When the stress determination was carried out by means of the Etchecopar et al. [1981] method, the stress ellipsoid shape ratio  $R=(\sigma_2-\sigma_3)/(\sigma_1-\sigma_3)$  was also calculated (stations 1-23 and 32-42). When stress determination was carried out by means of graphical methods, then only the principal stress directions of  $\sigma_1$  and  $\sigma_3$  were specified (stations 24-31). The last two columns in Table 3 indicate additional parameters such as (1) the quality factor  $QF$ , which indicates the quality of the stress determination (A, B, and C correspond to good, medium, and poor quality stress results, respectively); (2) the number of microtectonic data constraining the stress tensor solution (NMD); and (3) the local tectonic deformation phase corresponding to the calculated stress tensor (LTP). The complete data set and the stress analysis for the studied outcrops are summarized in supplemental figures (Appendix B). The Etchecopar et al. method is based on the minimization of angular differences between calculated and observed striae along microfaults, supposing that the stress tensor is homogeneous at the outcrop scale and that tectonic deformation remains low. Each frame in the supporting figures in Appendix B displays the stereographic projection of faults used in the determination of the stress tensor (big stereoplot) with the observed and calculated striae. The small stereoplot shows the microfault data that were rejected during the inversion process. The normalized Mohr circle diagram and the histogram of angular deviations are also shown.

In Figure 5 the horizontal projections of the compressional stress axes ( $\sigma_1$ ) are plotted for all available solutions. The orientation of the compressional axis in the Bucaramanga seismicity nest is also indicated. In outcrops 1-33, 35, 37, 39, and 40, one single deformation phase was observed; in the remaining outcrops, which are all located in the Bucaramanga sector (outcrops 34, 36, 38, 41, and 42), two deformation phases resulted from the analysis. Notice that in several outcrops the measurements were done on steeply dipping beds (Table 3). In these cases, the dip of the compressional axis is always much lower, indicating that the measured microfaults occurred during the final stages of tilting and folding of sedimentary rocks.

The results corresponding to the region north of Tunja (stations 22-32), in the axial zone of the EC, indicate a rather homogeneous E-SE compressive regime (N125°E). Other tectonic and geomorphologic features such as N30°E trending thrusts and folds present in this region are in agreement with this result. In the eastern foothill region (stations 7-12), stress results indicate again an E-SE compression direction (N120°E). These observations are consistent with thrusting along the Piedemonte Llanero fault system (PLFS) and with focal mechanisms (e.g., Tauramena earthquake, Table 2, and Plate 4).

The principal stress directions obtained in the Bogotá zone

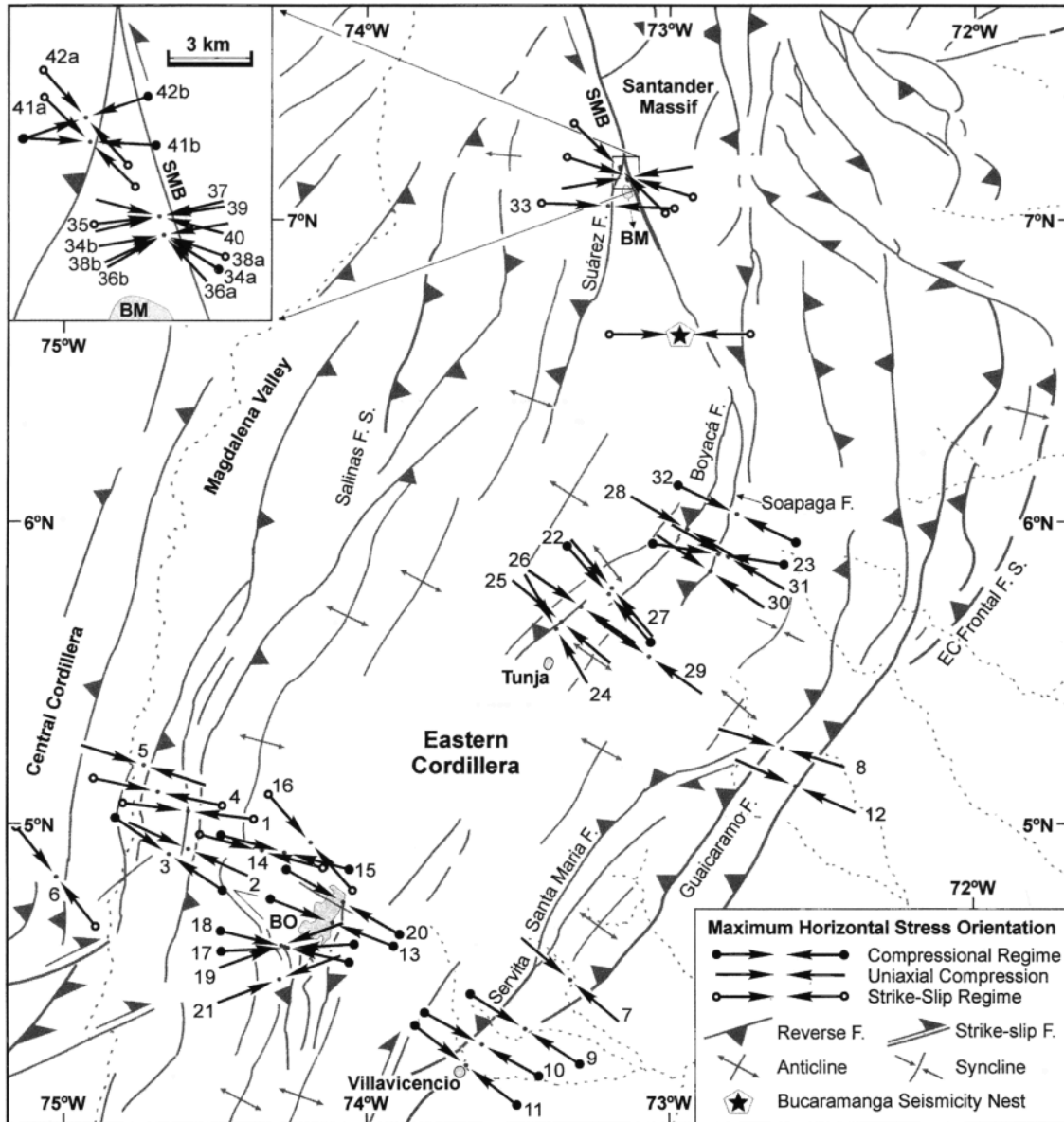


**Figure 5.** Neotectonic stress map of the northern half of the EC. Stress tensors were calculated in 42 different sites from microtectonic observations (Table 3). Arrows indicate the main horizontal compressional axis. The upper left inset shows stress results near the intersection between the Santa Marta – Bucaramanga and Suárez faults (near Bucaramanga, BM). The orientation of the compressional stress axis in the Bucaramanga seismicity nest is indicated. BO, Bogotá; FS, fault system.

(stations 13-21) are more complex. A global E-SE direction is still observed, yet some stations show directions ranging from NW-SE to NE-SW. The deviations that are observed in stations 16-18 could be associated with the presence of Neogene NW left-lateral transpressive faulting. Stations 19 and 21 show an ENE-WSW compression that could correspond to a pre-Andean transpressive phase. These outcrops (excepting station 16) are located southward of Bogotá, near the intersection between the Facatativa strike-slip fault and N-S trending thrusts.

Farther west, in the Magdalena valley area, stress analysis results (stations 1-5) turn slightly counterclockwise (the

orientation of  $\sigma_1$  is close to N110°E). A similar rotation is also observed in the directions of the tectonic and morphological main structures (e.g., Salinas thrust).

In the Bucaramanga sector (stations 33-42) where two major fault systems converge (SMB and Suárez faults), two types of solutions were observed: (1) a N80°E compression which is sub-orthogonal to the SMB fault and (2) a NW-SE compression. The stress determination in Plio-Quaternary sedimentary rocks (stations 34-37) indicates a well-constrained uniaxial compression with  $\sigma_1$  close to N80°E (solutions 34b, 35, 36b, and 37). We interpret these results as corresponding to the late

Table 3. Results of Microtectonic Stress Analysis in the Eastern Cordillera

St	Long	Lat	Lithology	Age	Strat	$\sigma_1$	$\sigma_2$	$\sigma_3$	R	QF, NMD	LTP
1	-74.53°	5.03°	limestone	E. Cretaceous	112°,32°S	277°,10°	022°,57°	181°,31°	0.52	A, 16	Early Andean
2	-74.53°	4.90°	calc. siltstone	E. Cretaceous		114°,07°	002°,69°	204°,19°	0.10	A, 19	Andean
3	-74.59°	4.88°	cong. sandstone	E. Tertiary	045°,38°W	304°,01°	034°,29°	212°,61°	0.46	A, 13	Andean
4	-74.63°	5.09°	conglomerate	E. Tertiary	006°,18°E	282°,22°	135°,65°	017°,12°	0.57	A, 18	Andean
5	-74.67°	5.18°	cong. sandstone	E. Tertiary	014°,40°E	108°,36°	241°,43°	357°,26°	0.01	B, 7	Andean
6	-74.95°	4.81°	granodiorite	Jurassic		142°,37°	315°,53°	049°,03°	0.74	A, 24	Early Andean?
7	-73.31°	4.44°	sandstone	Neogene	064°,47°N	311°,17°	161°,71°	044°,09°	0.00	A, 16	Andean
8	-72.64°	5.23°	sandstone	E. Cretaceous		287°,25°	181°,30°	049°,49°	0.14	A, 17	Andean
9	-73.45°	4.28°	mudstone	Neogene		123°,01°	033°,01°	262°,89°	0.57	A, 9	Andean
10	-73.59°	4.22°	mudstone	Plio-Quaternary		119°,05°	026°,29°	219°,61°	0.34	A, 10	Late Andean
11	-73.64°	4.15°	sandstone	E. Cretaceous		128°,26°	222°,09°	329°,63°	0.84	A, 10	Andean
12	-72.60°	5.10°	gravel	Quaternary		114°,36°	003°,26°	245°,43°	0.04	A, 10	Late Andean
13	-74.08°	4.65°	mudstone	E. Tertiary	023°,54°E	111°,27°	212°,20°	333°,56°	0.49	A, 15	Andean
14	-74.29°	4.90°	siltstone	L. Cretaceous	000°,40°E	285°,11°	100°,79°	195°,01°	0.75	A, 19	Andean
15	-74.23°	4.88°	siltstone	L. Cretaceous	020°,44°E	105°,11°	012°,18°	225°,69°	0.29	A, 16	Andean
16	-74.14°	4.92°	siltstone	L. Cretaceous		319°,19°	090°,62°	222°,20°	0.83	B, 9	Andean
17	-74.22°	4.56°	sandstone	L. Cretaceous	019°,45°E	087°,14°	351°,26°	203°,60°	0.38	A, 16	Early Andean
18	-74.23°	4.57°	siltstone	L. Cretaceous	023°,45°S	104°,13°	195°,04°	303°,77°	0.50	A, 8	Andean
19	-74.24°	4.57°	sandstone	L. Cretaceous	150°,50°E	070°,07°	161°,05°	282°,81°	0.23	A, 14	Pre-Andean
20	-74.04°	4.72°	lagoonal deposit	Quaternary		300°,05°	030°,03°	153°,84°	0.41	A, 19	Late Andean
21	-74.24°	4.46°	siltstone	L. Cretaceous	015°,45°E	069°,24°	162°,07°	267°,65°	0.08	A, 16	Pre-Andean
22	-73.18°	5.76°	siltstone	Paleogene		139°,02°	048°,23°	234°,67°	0.49	A, 10	Andean
23	-72.84°	5.90°	conglomerate	Jurassic	162°,51°W	279°,05°	186°,28°	018°,61°	0.78	B, 8	Andean
24	-73.35°	5.64°	siltstone	L. Cretaceous	064°,35°E	150°,00°		060°,90°		A, 15	Andean
25	-73.33°	5.67°	siltstone	L. Cretaceous	043°,30°N	130°,00°		040°,90°		B, 12	Andean
26	-73.27°	5.72°	siltstone	L. Cretaceous	030°,40°N	124°,00°		034°,90°		B, 10	Andean
27	-73.17°	5.78°	sandstone	Jurassic	050°,15°N	140°,00°		050°,90°		B, 10	Andean
28	-72.94°	5.98°	sandstone	E. Cretaceous	035°,35°N	120°,00°		030°,90°		B, 8	Andean
29	-73.06°	5.55°	sandstone	Paleogene	029°,34°W	305°,30°		125°,60°		B, 8	Andean
30	-72.86°	5.84°	limestone	E. Cretaceous	030°,52°W	124°,00°		034°,90°		B, 12	Andean
31	72.81°	5.89°	sandstone	E. Cretaceous	010°,39°E	120°,00°		030°,90°		B, 8	Andean
32	-72.78°	6.03°	cataclastic	Paleozoic		296°,02°	026°,13°	197°,77°	0.35	B, 7	Andean
33	-73.18°	7.08°	sandstone	Cretaceous ?		092°,12°	199°,54°	354°,33°	0.68	A, 10	Late Andean
34a	-73.12°	7.16°	gravel	Plio-Quaternary		302°,16°	211°,02°	116°,74°	0.69	B, 9	Andean
34b	-73.12°	7.16°	gravel	Plio-Quaternary		260°,00°	350°,00°	119°,90°	0.09	A, 15	Late Andean
35	-73.12°	7.17°	gravel	Plio-Quaternary		263°,08°	117°,80°	353°,06°	0.44	A, 12	Late Andean
36a	-73.12°	7.16°	gravel	Plio-Quaternary		317°,35°	092°,45°	209°,24°	0.15	B, 7	Andean
36b	-73.12°	7.16°	gravel	Plio-Quaternary		060°,06°	329°,08°	189°,80°	0.04	A, 15	Late Andean
37	-73.12°	7.17°	gravel	Plio-Quaternary		256°,07°	356°,56°	161°,33°	0.02	A, 9	Late Andean
38a	-73.12°	7.16°	limestone	Paleozoic		109°,09°	351°,72°	201°,15°	0.34	A, 11	Andean
38b	-73.12°	7.16°	limestone	Paleozoic		245°,34°	054°,55°	152°,05°	0.17	A, 8	Late Andean
39	-73.12°	7.17°	limestone	Paleozoic		261°,18°	357°,19°	132°,63°	0.05	A, 27	Late Andean
40	-73.12°	7.17°	limestone	Paleozoic		285°,21°	069°,65°	190°,13°	0.06	A, 18	Andean
41a	-73.14°	7.20°	limestone	Paleozoic		137°,17°	011°,63°	233°,21°	0.32	A, 20	Andean
41b	-73.14°	7.20°	limestone	Paleozoic		093°,04°	002°,12°	200°,77°	0.29	A, 11	Late Andean
42a	-73.14°	7.21°	limestone	Paleozoic		140°,34°	290°,52°	040°,15°	0.49	B, 5	Andean
42b	-73.14°	7.21°	limestone	Paleozoic		070°,12°	162°,09°	286°,75°	0.26	A, 9	Late Andean

The stress axes are specified by means of the azimuth and the dip angle. The bedding plane is specified by means of the azimuth, the dip, and the geographical quadrant of the dip. Azimuths are measured clockwise from the north; dips are measured downward from the horizontal. St, microtectonic station; Long, longitude; Lat, latitude; Strat, bedding plane; R=( $\sigma_2$ - $\sigma_3$ )/( $\sigma_1$ - $\sigma_3$ ); QF, quality factor for the stress tensor solution (A, good; B, medium; C, poor); NMD, number of microtectonic data constraining the stress tensor solution; LTP, local tectonic phase. Cong., conglomeratic; E., early; L., late. See Figure 5 and Appendix B.

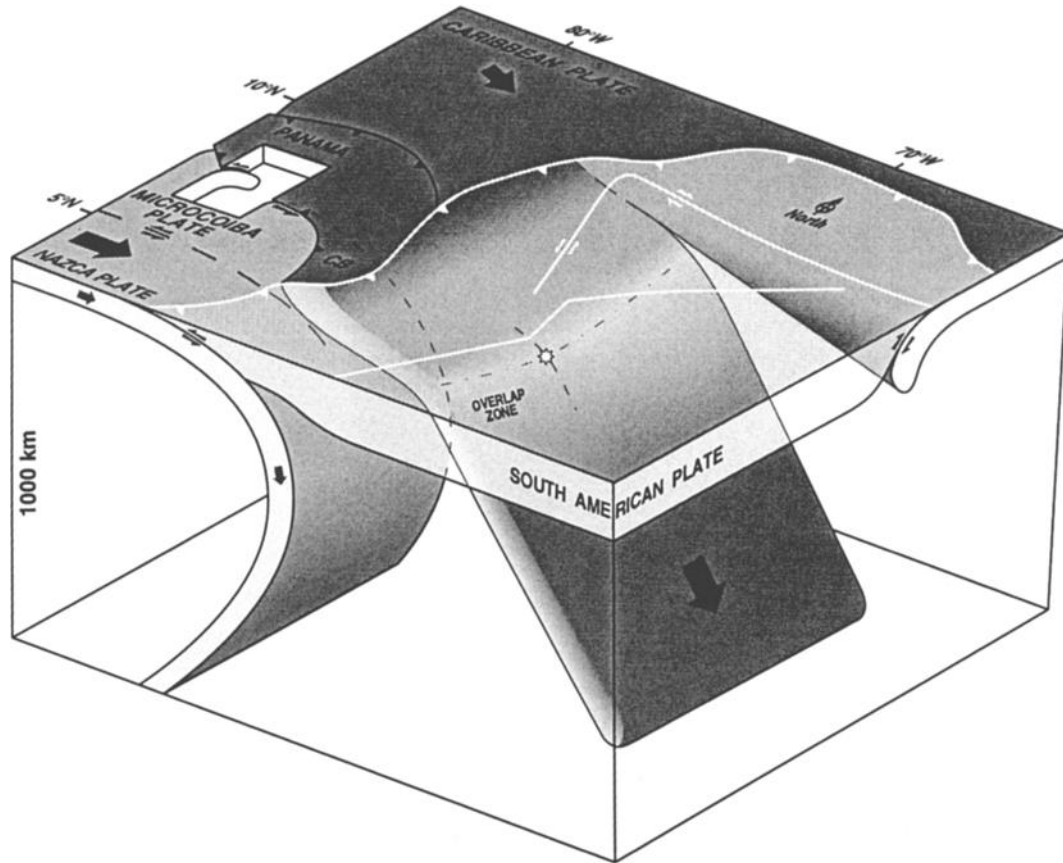


**Figure 6.** Schematic block diagram indicating the three-dimensional geometry and kinematics of the oceanic subductions beneath the northern Andes. The Bucaramanga seismicity nest is indicated by the white star located in the paleo-Caribbean plate. The main intracontinental fault systems and the South Caribbean Marginal fault are indicated in white; the thrust located along the Colombian Nazca trench and the suture between the Chocó block (CB) and the Western Cordillera are also indicated in white (Plate 1). Fault systems in black affect the oceanic plates. The overlap zone located between 5.2°N and 7°N corresponds to a region where both the Nazca and paleo-Caribbean plate are present.

Andean tectonic phase in the Bucaramanga area. This compressional axis is coherent with other regional stress indicators such as shallow focal mechanisms in the Santander Massif (SM) (e.g., mechanisms 4, 8, 27, and 28, Plate 4). Solutions 34a and 36a were obtained from the analysis of fault slip data that were not compatible with the N80°E compressive phase. The obtained tensors are less well constrained and are compatible with a NW-SE compression, which we interpret as the tectonic regime that prevailed during the early Andean phase. Stations 38-42, located in Paleozoic rocks, indicate stress tensor solutions with a compressional direction ranging from NW-SE to N70°E. Stations 38, 41, and 42 show the two deformation phases mentioned previously. Solutions 38a, 41a, and 42a indicate an average NW-SE strike-slip regime, which we interpret as early Andean. Solutions 38b, 39, 41b, and 42b indicate an average N80°E uniaxial compression. Station 40 shows a uniaxial compression oriented N105°E, which is intermediate between the two tectonic phases determined in other stations.

The occurrence of two tectonic phases in the Bucaramanga zone can be related to the migration of tectonic deformation in the EC during the Andean phase. The NW-SE compressional direction is coherent with left-lateral movement along the

southern segment of the SMB fault and thrusting along the Boyacá and Soapaga faults during the early Andean (Figure 5). The N80°E compressional direction is coherent with active thrusting along the western flank of the EC: the azimuth of the Suárez and Salinas faults near Bucaramanga is close to N-S (Plate 1). The SMB fault shows several evidences of recent left-lateral movement in the Bucaramanga sector, such as triangular facets and deviations of the drainage network parallel to the fault trace; notice that recent faulting has occurred within a tectonic stress field characterized by a  $\sigma_1$  direction that is sub-orthogonal to the fault. The orientation of the stress tensor axes implies that the tectonic shear stress along the main fault is low. This observation suggests that the mechanical behavior of the SMB fault during the late Andean phase might have corresponded to a weak fault (characterized by a low friction value).

These stress results are globally coherent with the Neogene E-SE convergence between the PCP and NWSA. Nevertheless, they should be completed by more measurements of stress and kinematic indicators, in particular, in areas where information is lacking (e.g., SM and Magdalena valley) and in complex areas such as the southern termination of the SMB fault and the Bogotá zone.

## 6. Conclusions

The complex geodynamics of the northern Andes is characterized by the subduction of the PCP and the Nazca plate beneath NWSA. The block diagram in Figure 6 indicates the hypothetical geometry and kinematics of the subducting oceanic plates; the main geodynamic features are the following: (1) A shallow ~N-NE trending subduction of the PCP, northward of 5.2°N to 5.5°N. The PCP possibly plunges into the mantle beneath the EC and the Maracaibo block to a depth of around 1000 km. A tear fault may exist in the PCP along the San Sebastian-El Pilar fault system in Venezuela. (2) A moderately steep ~N-S trending subduction of the Nazca plate southward of 7°N. The Nazca plate plunges into the mantle beneath the CC and possibly overturns in the lower mantle. The northern boundary of the plate is transpressive and subduces locally beneath Panama. (3) An overlap region between the PCP and the Nazca plate, between 5.2°N and 7°N.

The interaction between the two subducting plates in the overlap region creates active faulting in both slabs. The eastward movement of the Nazca plate “pushes” the PCP, creating deformation along roughly E-W trending fault zones that bound the overlap region:

1. Intermediate seismicity distribution beneath the EC suggests the existence of a major right-lateral transform shear zone located at around 5.2°N, with azimuth between N90°E and N100°E. This fault aligns itself with the southern termination of the Baudó Range and may be considered as the southern limit of the PCP. The southern limit of the Coiba microplate, located at around 5.5°N, is also aligned with this transform shear zone and shows active left-lateral movement.

2. The Bucaramanga seismicity nest located in the PCP at a depth of 150 km (at 6.8°N, 73°W) may correspond to an inflexion zone or a “hinge” zone in the oceanic slab.

Intracontinental deformation in the northern Andes results from oblique convergence between the oceanic slabs and NWSA. The transpressive tectonic phases observed in the Colombian Cordilleras may be linked to (1) the accretion/collision episodes that occurred along the active margin of NWSA during the Cenozoic; (2) the NE to E-NE trending motion between the oceanic slabs (Farallon and PCP) and the Cordilleras during the Paleogene; and (3) the E-W convergence between the Nazca plate and NWSA and the E-SE convergence between the PCP and NWSA, during Neogene.

Neogene intracontinental deformation northward of 5°N is mainly influenced by the E-SE convergence between the PCP and NWSA. The IDZ and the Ibagué right-lateral fault zone in the south and the Santa Marta-Bucaramanga (SMB) left-lateral fault to the northeast are the boundaries of a deformable continental wedge that is moving toward the E-SE. This block seems to be dragged by the PCP located beneath. Progressive movement of the wedge is absorbed along reverse faults located in the foothills of the three Cordilleras and, in particular, in the EC. Notice that the Garrapatas and Ibagué “en echelon” faults are slightly shifted southward relative to the PCP shear zone located at 5.2°N (Plate 1).

Crustal seismicity in the Colombian Andes is well correlated with the main tectonic features observed at the surface, in particular, with active fault systems situated along the eastern and

western foothills of the EC and with faulting in the Central and Western Cordilleras north of Buenaventura. Our results suggest that the northern Eastern Cordillera results from shortening of a thinned and weakened continental lithosphere linked to active subduction of the PCP beneath the range (the oceanic slab strikes N30°E and dips between 30° and 60° toward the craton). Two regional cross sections from the Magdalena valley through the Eastern Cordillera to the Llanos Basin (across the Tunja and Bucaramanga areas) support this interpretation. The subduction zone shows a dominant reverse movement coherent with N-NE trending thrusts and folds observed in the crust (Plate 1). Total shortening in this area during Cenozoic compressional events is ~120 km.

Stress tensor determinations from fault slip data in the northern segment of the EC are in agreement with an homogeneous E-SE compressive regime during the Andean tectonic phase. Results around Bucaramanga, where two major fault systems converge (SMB and Suárez faults), indicate a late Andean N80°E uniaxial compression which is suborthogonal to the SMB fault. A change of orientation of stress directions may be found along the EC. Namely, southward of Villavicencio, folding and faulting are compatible with a principal stress  $\sigma_1$  oriented in the EW direction (e.g., Macarena range). Nevertheless,  $\sigma_1$  rotates and takes an E-SE direction northward of the Algeciras fault. The stress results obtained in the EC may be incorporated in mechanical models of the stress field in NWSA [e.g., Meijer, 1995].

The Maracaibo triangular block is bounded by the SMB and Oca-Ancón conjugate strike-slip fault systems and by the Andes de Mérida range. Compressional deformation in the Andes de Mérida, the Perijá range, and the Sierra Nevada de Santa Marta is also coherent with E-SE convergence between the PCP and NWSA. The Maracaibo block exhibits right-lateral movement along the Boconó fault, which is located along the axial zone of the Andes de Mérida and trends N50°E. Shortening and lateral expulsion of the Maracaibo block are driven by E-SE movement of the PCP and by convergence of the previously mentioned continental wedge. Intracontinental subduction beneath the Andes de Mérida range [Colletta *et al.*, 1997] might also result from shortening of thinned and weakened continental lithosphere, linked to the indentation of the Maracaibo block, and should display a right-lateral component.

**Acknowledgments.** The authors are grateful to G. París, H. Vergara, C. Ulloa, G.C. Renzoni, C. Dimaté, A. Sarria, J. P. Soulas, E. Castro, J. Romero, G. Camargo, G. Fajardo, J. Zúñiga, E. Carrillo, J. Clavijo, and geologists of INGEOMINAS, Ecopetrol, and Carder, with whom we shared field trips and discussions on Andean tectonics in the past 10 years. We would like to thank H. Salamanca, N. Prada, W. Ruiz, J. Escallón, and C. Montoya of the Universidad de Los Andes, and A. Delplanque of the Université de Montpellier, for technical help. We are also grateful to M. Mattauer, A. Chemenda, J. Ritz, J. Malavieille, M. Séranne, S. Lallemand, J.M. Dautria, and Y. Branquet for discussions and observations on the manuscript, and to M.A. Gutscher for comments on the manuscript and for correcting the English. Reviewer's comments greatly improved the manuscript. This work was supported by the Universidad de Los Andes (Bogotá), the Instituto de Investigaciones en Geociencias, Minería y Química (Bogotá), the Ecopetrol Exploration Division (Bogotá), the Université de Montpellier II (UMR 5573), the Institut de Physique du Globe de Strasbourg, and the California Institute of Technology (Division Contribution 8715).

## References

- Alfonso, C., P. Sacks, D. Secor, J. Rine, and V. Perez, A tertiary fold and thrust belt in the Valle del Cauca basin, Colombian Andes, *J. S. Am. Earth Sci.*, **7**, 387-402, 1994.
- Aspden, J., and M. Litherland, The geology and Mesozoic collisional history of the Cordillera Real, Ecuador, *Tectonophysics*, **205**, 187-204, 1992.
- Aspden, J., W. McCourt, and M. Brook, Geometrical control of subduction-related magmatism: The Mesozoic and Cenozoic plutonic history of western Colombia, *J. Geol. Soc. London*, **144**, 893-905, 1987.
- Audemard, F., and A. Singer, Active fault recognition in northwestern Venezuela and its seismogenic characterisation: Neotectonic and paleoseismic approach, *Geofis. Int.*, **35**, 245-255, 1996.
- Baldock, J., Geology of Ecuador: Explanatory bulletin of the national geological map of the Republic of Ecuador, scale 1:1,000,000, Min. Rec. Nat. Energ., Quito, 1982.
- Beltrán, C., Mapa neotectónica de Venezuela, scale 1:2,000,000, Funvisis, Caracas, 1993.
- Bijwaard, H., W. Spakman, and R. Engdahl, Closing the gap between regional and global travel time tomography, *J. Geophys. Res.*, **103**, 30,055-30,078, 1998.
- Boinet, T., J. Bourgeois, H. Mendoza, and R. Vargas, La falla de Bucaramanga (Colombia): Su función durante la orogénia andina, *Geol. Norandina*, **11**, 3-10, 1989.
- Branquet, Y., B. Laumonier, A. Cheilletz, and G. Giuliani, Emeralds in the Eastern Cordillera of Colombia: Two tectonic settings for one mineralization, *Geology*, **27**, 597-600, 1999.
- Case, J., T. Holcombe, and R. Martin, Map of geologic provinces in the Caribbean region, *Mem. Geol. Soc. Am.*, **162**, 30 pp., 1984.
- Casero, P., J. Salel, and A. Rossato, Multidisciplinary correlative evidences for polyphase geological evolution of the foot-hills of the Cordillera Oriental (Colombia), paper presented at VI Simposio Bolivariano, Exploración Petrolera en las Cuencas Sub-Andinas, Asoc. Colombiana Geólogos Geofísicos Petróleo, Cartagena, Colombia, 1997.
- Colletta, B., F. Hebrard, J. Letouzey, P. Werner, and J. Rudkiewicz, Tectonic style and crustal structure of the Eastern Cordillera (Colombia) from a balanced cross section, in *Petroleum and Tectonics in Mobile Belts*, edited by J. Letouzey, pp. 81-100, Technip, Paris, 1990.
- Colletta, B., F. Roure, B. De Toni, D. Loureiro, H. Passalacqua, and Y. Gou, Tectonic inheritance, crustal architecture, and contrasting structural styles in the Venezuela Andes, *Tectonics*, **16**, 777-794, 1997.
- Cooper, B., et al., Basin development and tectonic history of the Eastern Cordillera and Llanos Basin, Colombia, *AAPG Bull.*, **79**, 1421-1443, 1995.
- Corredor, F., Evidences for a passive roof duplex along the northeastern thrust front of the Eastern Cordillera, Colombia and implications for oil exploration, paper presented at VI Simposio Bolivariano, Exploración Petrolera en las Cuencas Sub-Andinas, Asoc. Colombiana Geólogos Geofísicos Petróleo, Cartagena, Colombia, 1997.
- de Boer, J. Z., M. Defant, R. Stewart, J. Restrepo, L. Clark, and A. Ramirez, Quaternary calc-alkaline volcanism in western Panama: Regional variation and implication for the plate tectonic framework, *J. S. Am. Earth Sci.*, **1**, 275-293, 1988.
- de Boer, J. Z., M. Defant, R. Stewart, and H. Bellon, Evidence for active subduction below western Panama, *Geology*, **19**, 649-652, 1991.
- Dengo, C., and M. Covey, Structure of the Eastern Cordillera of Colombia: Implications for trap styles and regional tectonics, *AAPG Bull.*, **77**, 1315-1337, 1993.
- Dewey, J., Seismicity and tectonics of western Venezuela, *Bull. Seismol. Soc. Am.*, **62**, 1711-1751, 1972.
- Duque-Caro, H., Structural style, diapirism and accretionary episodes of the Sinu-San Jacinto terrane, southwestern Caribbean borderland, in *The Caribbean-South American Plate Boundary and Regional Tectonics*, edited by W. Bonini, R. Hargraves, and R. Shagam, *Mem. Geol. Soc. Am.*, **162**, 303-316, 1984.
- Duque-Caro, H., Neogene stratigraphy, paleoceanography and paleobiogeography in northwest South America and the evolution of the Panama Seaway, *Palaeogeogr. Palaeoclimatol. Palaeoecol.*, **77**, 203-234, 1990.
- Duque-Caro, H., The Chocó Block in the northwestern corner of South America: Structural, tectonostratigraphic, and paleogeographic implications, *J. S. Am. Earth Sci.*, **3**, 71-84, 1990b.
- Engdahl, E., R. van der Hilst, and R. Buland, Global teleseismic earthquake relocation with improved travel times and procedures for depth relocation, *Bull. Seismol. Soc. Am.*, **88**, 722-743, 1998.
- Etayo, F., G. Renzoni, and D. Barrero, Contornos sucesivos del mar Cretáceo en Colombia, paper presented at Primer Congreso Colombiano de Geología, INGEOMINAS, Bogotá, 1969.
- Etchecopar, A., G. Vasseur, and M. Daignières, An inverse problem in microtectonics for the determination of stress tensors from fault striation analysis, *J. Struct. Geol.*, **3**, 51-65, 1981.
- Freymueller, J., J. Kellogg, and V. Vega, Plate motions in the North Andean Region, *J. Geophys. Res.*, **98**, 21,853-21,863, 1993.
- Gordon, R., and D. Jurdy, Cenozoic global plate motions, *J. Geophys. Res.*, **91**, 12,389-12,406, 1986.
- Grösser, J., Geotectonic evolution of the Western Cordillera of Colombia: New aspects from geochemical data on volcanic rocks, *J. S. Am. Earth Sci.*, **2**, 359-369, 1989.
- Gutscher, M.A., J. Olivet, D. Aslanian, J. Eissen, and R. Maury, The "lost Inca plateau": Cause of flat subduction beneath Peru?, *Earth Planet. Sci. Lett.*, **171**, 335-341, 1999.
- Guzmán, J., G. Franco, M. Ochoa, G. Paris, and A. Taboada, Proyecto para la mitigación del riesgo sísmico de Pereira, Dosquebradas y Santa Rosa de Cabal: Evaluación neotectónica, Informe Final, Corporación Autónoma Regional de Risaralda, Pereira, Colombia, 1998.
- Helmens, K., and T. Van der Hammen, Memoria explicativa de los mapas del neógeno y cuaternario de la sabana de Bogotá-cuenca alta del río Bogotá, *Anál. Geogr.*, **24**, pp. 91-142, Instituto Geográfico Agustín Codazzi, Bogotá, 1995.
- Hey, R., Tectonic evolution of the Cocos - Nazca spreading center, *Geol. Soc. Am. Bull.*, **88**, 1404-1420, 1977.
- INGEOMINAS, Atlas geológico digital de Colombia, map, sheets 1-18, scale 1:500,000, Bogotá, 1997.
- Irving, E., La evolución estructural de los Andes mas septentrionales de Colombia, *Bol. Geol. Colomb. Inst. Nac. Invest. Geol. Min.*, **19** (2), 90 pp., 1971.
- Julivert, M., La morfoestructura de la zona de mesas al SW de Bucaramanga, Colombia, *Bol. Geol.*, **1**, pp. 7-43, Univ. Ind. de Santander, Bucaramanga, Colombia, 1958.
- Kammer, A., Steeply dipping basement faults and associated structures of the Santander Massif, Eastern Cordillera, Colombian Andes, *Geol. Colomb.*, **18**, 47-64, 1993.
- Kanamori, H., and K. McNally, Variable rupture mode of the subduction zone along the Ecuador-Colombia coast, *Bull. Seismol. Soc. Am.*, **72**, 1241-1253, 1982.
- Kay, S., Changing slab dip and the Neogene magmatic / tectonic evolution of the central Andean arc, paper presented at 4<sup>th</sup> International Symposium on Andean Geodynamics, Institut de Recherche pour le Développement, Göttingen, 1999.
- Keller, G., C. Zenker, and S. Stone, Late Neogene history of the Pacific-Caribbean gateway, *J. S. Am. Earth Sci.*, **2**, 73-108, 1989.
- Kellogg, J., and W. Bonini, Subduction of the Caribbean plate and basement uplifts in the overriding South American plate, *Tectonics*, **1**, 251-276, 1982.
- Kellogg, J., and H. Duque, Crustal scale deformation in the Eastern Cordillera, Colombia, paper presented at V Simposio Bolivariano, Exploración Petrolera en las Cuencas Subandinas, Sociedad Venezolana de Geólogos, Puerto de La Cruz, Venezuela, 1994.
- Kellogg, J., and V. Vega, Tectonic development of Panama, Costa Rica, and the Colombian Andes: Constraints from Global Positioning System geodetic studies and gravity, *Spec. Pap. Geol. Soc. Am.*, **295**, 75-90, 1995.
- Ladd, J., Relative motion of South America with respect to North America and Caribbean tectonics, *Geol. Soc. Am. Bull.*, **87**, 969-976, 1977.
- Lahr, J. C., HYPOELLIPSE: A computer program for determining local earthquakes, hypocentral parameters, magnitude and first motion pattern, *Open File Rep. 79-0431*, 313 pp., U.S. Geol. Surv., 1985.
- Laubscher, H.P., The kinematic puzzle of the Neogene northern Andes, in *The Anatomy of Mountain Ranges*, edited by J.P. Schaer and J. Rodgers, pp. 211-227, Princeton Univ. Press, Princeton, N.J., 1987.
- Lavenu, A., T. Winter, and F. Dávila, A Pliocene-Quaternary compressional basin in the Interandean Depression, central Ecuador, *Geophys. J. Int.*, **121**, 279-300, 1995.
- Lee, W., and J. C. Lahr, Hypo71 (revised): A computer program for determining hypocenter, magnitude, and first motion pattern of local earthquakes, *Open File Rep. 75-0311*, 59 pp., U.S. Geol. Surv., 1975.
- Lonsdale, P., and K. Klitgord, Structure and tectonic history of the Eastern Panama Basin, *Geol. Soc. Am. Bull.*, **89**, 981-999, 1978.
- MacKay, M. E., and G. F. Moore, Variation in deformation of the south Panama accretionary prism: Response to oblique subduction and trench sediment variation, *Tectonics*, **9**, 683-698, 1990.
- Malavé, G., and G. Suárez, Intermediate-depth seismicity in northern Colombia and western Venezuela and its relationship to Caribbean plate subduction, *Tectonics*, **14**, 617-628, 1995.
- Malavieille, J., and A. Chemenda, Impact of initial geodynamic setting on structure, ophiolite emplacement and tectonic evolution of collisional belts, *Ophiolit.*, **22**, 3-13, 1997.
- Mann, P., and K. Burke, Neotectonics of the Caribbean, *Rev. Geophys.*, **22**, 309-362, 1984.
- Mann, P., and J. Corrigan, Model for late Neogene deformation in Panama, *Geology*, **18**, 558-562, 1990.
- Martínez, A., Géologie de la région d'Iza, Boyacá: Cordillère Orientale de Colombie, memoir, 34 pp., *Inst. Mineral. et Geol.*, Univ. de Lausanne, Dorigny, Switzerland, 1989.
- Mauffret, A., and S. Leroy, Seismic stratigraphy and structure of the Caribbean igneous province, *Tectonophysics*, **283**, 61-104, 1997.
- McCourt, W., J. Aspden, and M. Brook, New geological and geochronological data from the Colombian Andes: Continental growth by multiple accretion, *J. Geol. Soc. London*, **141**, 831-845, 1984.
- Mégard, F., Cordilleras Andes and Marginal Andes: A review of Andean geology north of the Arica Elbow (18°S), *Geodyn. Ser.*, **18**, 71-95, 1987.
- Meijer, P., Dynamics of active continental margins:

- The Andes and the Aegean region, *Ph.D. thesis*, 218 pp., Utrecht Univ., Utrecht, Netherlands, 1995.
- Mojica, J., A. Kammer, and G. Ujueta, El jurásico del sector noroccidental de Suramérica y guía de la excursión al Valle Superior del Magdalena (Nov. 1-4/95), Regiones de Payandé y Prado, Departamento del Tolima, Colombia, *Geol. Colomb.*, 21, 3-40, 1996.
- Morales, L., and Colombian Petroleum Industry, General geology and oil occurrences of Middle Magdalena Valley, Colombia, in *Habitat of Oil*, edited by L. Weeks, pp. 641-695, Am. Assoc. Petrol. Geol., Tulsa, Oklahoma, 1958.
- Paris, G., and J. Romero, Fallas activas en Colombia: Mapa neotectónico preliminar, *Bol. Geol.* 34, 42 pp. and map, INGEOMINAS, Bogotá, 1994.
- Pennington, W., Subduction of the Eastern Panama Basin and seismotectonics of northwestern South America, *J. Geophys. Res.*, 86, 10,753-10,770, 1981.
- Pérez, O., M. Jaimés, and E. Garcíacaro, Microseismicity evidence for subduction of the Caribbean plate beneath the South American plate in northwestern Venezuela, *J. Geophys. Res.*, 102, 17,875-17,882, 1997.
- Pilger, R. H., Jr., Kinematics of the South American subduction zone from global plate reconstructions, in *Geodynamics of the Eastern Pacific Region, Caribbean and Scotia Arcs, Geodyn. Ser.*, vol. 9, edited by S.J. Cabré, pp. 113-126, AGU, Washington, D.C., 1983.
- Pindell, J., and S. Barrett, Caribbean plate tectonic history, in *The Caribbean Region*, edited by G. Dengo, and J. Case, *The Geology of North America*, vol. H, pp. 405-432, Geol. Soc. of Am., Boulder, Colo., 1990.
- Renzoni, G., et al., Tunja, mapa geológico, sheet 191, scale 1:100,000, INGEOMINAS, Bogotá, 1983.
- Restrepo-Pace, P., Pliotectonic characterization of the Central Andean Terrane, Colombia, *J. S. Am. Earth Sci.*, 5, 97-116, 1992.
- Ritz, J., and A. Taboada, Revolution stress ellipsoids in brittle tectonics resulting from an uncritical use of inverse method, *Bull. Soc. Geol. Fr.*, 164, 519-531, 1993.
- Rivera, L. A., Inversion du tenseur de contraintes à partir des données de polarité pour une population de séismes: Application au Nid de Bucaramanga, *Ph.D. thesis*, 266 pp., Inst. Phys. Globe, Strasbourg, France, 1989.
- Rosencrantz, E., M. Ross, and J. Sclater, Age and spreading history of the Cayman trough as determined from depth, heat flow, and magnetic anomalies, *J. Geophys. Res.*, 93, 2141-2157, 1988.
- Santo, T., Characteristics of seismicity in South America, *Univ. Tokyo Earthquake Res. Inst. Bull.*, 47, 635-672, 1969.
- Silver, E., D. Reed, J. Tagudin, and D. Heil, Implications of the north and south Panama thrust belts for the origin of the Panama orocline, *Tectonics*, 9, 261-281, 1990.
- Sinton, C., R. Duncan, M. Storey, J. Lewis, and J. Estrada, An oceanic flood basalt province within the Caribbean plate, *Earth Planet. Sci. Lett.*, 155, 221-235, 1998.
- Soulas, J. P., Neotectónica y tectónica activa en Venezuela y regiones vecinas, paper presented at VI Congreso Geológico Venezolano, Sociedad Venezolana de Geólogos, Caracas, 1986.
- Stéphan, J. F., Andes et chaîne Caraïbe sur la transversale de Barquisimeto (Vénézuéla): Evolution géodynamique, paper presented at Géodynamique des Caraïbes, Symposium, Inst. Français du Pétrole, Paris, 1985.
- Steuer, M., P. Bentham, and G. Latimer, Structural style and emplacement of the Opón anticline, Middle Magdalena valley, Colombia, paper presented at VI Simposio Bolivariano, Exploración Petrolera en las Cuencas Sub-Andinas, Asoc. Colombiana Geólogos Geofísicos Petróleo, Cartagena, Colombia, 1997.
- Taboada, A., Stress and strain from striated pebbles: Theoretical analysis of striations on a rigid spherical body linked to a symmetrical tensor, *J. Struct. Geol.*, 15, 1315-1330, 1993.
- Taboada, A., C. Tournier, and P. Laurent, An interactive program for the graphical representation of striated faults and applied normal and tangential stress, *Comput. Geosci.*, 17, 1281-1310, 1991.
- Taboada, A., H. Salamanca, J. Zúñiga, and G. Fajardo, Modelación tectónica (elementos finitos) del área de Tunja, paper presented at VII Congreso Colombiano de Geología, INGEOMINAS, Bogotá, 1996.
- Taboada, A., C. Dimaté, and A. Fuenzalida, Sismotectónica de Colombia: deformación continental activa y subducción, *Fis. Tierra Madrid*, 10, 111-147, 1998.
- Tibaldi, A., and L. Ferrari, Latest Pleistocene-Holocene tectonics of the Ecuadorian Andes, *Tectonophysics*, 205, 109-125, 1992.
- Toto, E., and J. Kellogg, Structure of the Sinu-San Jacinto fold belt: An active accretionary prism in northern Colombia, *J. S. Am. Earth Sci.*, 5, 211-222, 1992.
- Tschanz, C., R. Marvin, B. Cruz, H. Mehnert, and C. Cebulla, Geologic evolution of the Sierra Nevada de Santa Marta, northeastern Colombia, *Geol. Soc. Am. Bull.*, 85, 273-284, 1974.
- Ulloa, C., et al., Guateque, mapa geológico del cuadrángulo K-12, scale 1:100,000, INGEOMINAS, Bogotá, 1975.
- Ulloa, C., et al., Tauramena, mapa geológico, sheet 211, scale 1:100,000, INGEOMINAS, Bogotá, 1976.
- van der Hilst, R., and P. Mann, Tectonic implications of tomographic images of subducted lithosphere beneath northwestern South America, *Geology*, 22, 451-454, 1994.
- Vergara, H., Rasgos y actividad neotectónica de la falla de Algeciras, paper presented at VII Congreso Colombiano de Geología, INGEOMINAS, Bogotá, 1996.
- Vergara, H., A. Taboada, J. Romero, G. Paris, and E. Castro, Principales fuentes sísmogénicas de la región central de Colombia paper presented at VII Congreso Colombiano de Geología, INGEOMINAS, Bogotá, 1996.
- Wadge, G., and K. Burke, Neogene Caribbean plate rotation and associated Central American tectonic evolution, *Tectonics*, 2, 633-643, 1983.
- Ward, D., R. Goldsmith, A. Jimeno, J. Cruz, H. Restrepo, and E. Gómez, Bucaramanga, mapa geológico, sheet H-12, scale 1:100,000, INGEOMINAS, Bogotá, 1969.
- Ward, D., R. Goldsmith, L. Jaramillo, and R. Vargas, Pamplona, mapa geológico, sheet H-13, scale 1:100,000, INGEOMINAS, Bogotá, 1977.
- Wessel, P., and W. Smith, New, improved version of Generic Mapping Tools released, *Eos Trans. AGU*, 79(47), 579, 1998.
- Westbrook, G., N. Hardy, and R. Heath, Structure of the Panama-Nazca plate boundary, *Spec. Pap. Geol. Soc. Am.*, 295, 91-109, 1995.
- Wilson, M., *Igneous Petrogenesis: A Global Approach*, 466 pp., Unwin Hyman, Boston, Mass., 1989.
- Winter, T., J. P. Avouac, and A. Lavenue, Late Quaternary kinematics of the Pallatanga strike-slip fault (central Ecuador) from topographic measurements of displaced morphological features, *Geophys. J. Int.*, 115, 905-920, 1993.
- H. Bijwaard, Vening Meinesz School of Geodynamics, Institute of Earth Sciences, Utrecht University, Budapestlaan 4, 3584 CD Utrecht, Netherlands. (hbwd@cbs.nl)
- A. Cisternas, Institut de Physique du Globe, Université Louis Pasteur, 5 rue René Descartes, 67084 Strasbourg Cedex, France. (armando@sismo.u-strasbg.fr)
- A. Fuenzalida, now at Sipetrol Colombia, Calle 93B No. 17-25, Of. 410, Bogotá, Colombia. (AFUENZAL@sipetrol.com.co)
- J. Olaya, now at GAPS, Carrera 42 No. 167-79, Bogotá, Colombia. (jholaya@latinmail.com)
- H. Philip, and A. Taboada, Laboratoire de Géophysique, Tectonique, et Sédimentologie, CNRS-Université Montpellier 2, CC. 60, place E. Bataillon, 34095 Montpellier cédex 5, France. (philip@dstu.univ-montp2.fr; taboada@dstu.univ-montp2.fr)
- C. Rivera, INGEOMINAS, Diag. 53 No 34-53, Bogotá, Colombia.
- L.A. Rivera, Seismological Laboratory, California Institute of Technology, Pasadena, CA 91125. (luis@gps.caltech.edu)

(Received June 29, 1999;  
revised December 21, 1999;  
accepted January 10, 2000.)